Magnetic and glassy transitions in the square-lattice *XY* model with random phase shifts

J. Stat. Mech. (2010) P03006

(http://iopscience.iop.org/1742-5468/2010/03/P03006)

Journal of Statistical Mechanics: Theory and Experiment
An IOP and SISSA journal

Magnetic and glassy transitions in the square-lattice XY model with random phase shifts

Vincenzo Alba[1], **Andrea Pelissetto**[2] **and Ettore Vicari**[3]

[1] Scuola Normale Superiore and INFN, I-56126 Pisa, Italy
[2] Dipartimento di Fisica dell'Università di Roma 'La Sapienza' and INFN, I-00185 Roma, Italy
[3] Dipartimento di Fisica dell'Università di Pisa and INFN, I-56127 Pisa, Italy
E-mail: Vincenzo.Alba@sns.it, Andrea.Pelissetto@roma1.infn.it and Ettore.Vicari@df.unipi.it

Received 28 January 2010
Accepted 29 January 2010
Published 11 March 2010

Online at stacks.iop.org/JSTAT/2010/P03006
doi:10.1088/1742-5468/2010/03/P03006

Abstract. We investigate the magnetic and glassy transitions of the square-lattice XY model in the presence of random phase shifts. We consider two different random-shift distributions: the Gaussian distribution and a slightly different distribution (the cosine distribution) which allows the exact determination of the Nishimori line where magnetic and overlap correlation functions are equal. We perform Monte Carlo simulations for several values of the temperature and of the variance of the disorder distribution, in the paramagnetic phase close to the magnetic and glassy transition lines. We find that, along the transition line separating the paramagnetic and the quasi-long-range order phases, magnetic correlation functions show a universal Kosterlitz–Thouless behavior as in the pure XY model, while overlap correlations show a disorder dependent critical behavior. This behavior is observed up to a multicritical point which, in the cosine model, lies on the Nishimori line. Finally, for large values of the disorder variance, we observe a universal zero-temperature glassy critical transition, which is in the same universality class as that occurring in the gauge-glass model.

Keywords: classical Monte Carlo simulations, classical phase transitions (theory), critical exponents and amplitudes (theory), spin glasses (theory)

1742-5468/10/P03006+44$30.00

Contents

1. Introduction

The two-dimensional XY model with random phase shifts (RP XY) describes the thermodynamic behavior of several disordered systems, such as Josephson junction arrays with geometrical disorder [1, 2], magnetic systems with random Dzyaloshinskii–Moriya interactions [3], crystal systems on disordered substrates [4], and vortex glasses in high-T_c cuprate superconductors [5]. See [6, 7] for recent reviews. The RP XY model is defined by the partition function

$$Z(\{A\}) = \exp(-\mathcal{H}/T),$$
$$\mathcal{H} = -\sum_{\langle xy\rangle} \mathrm{Re}\,\bar{\psi}_x U_{xy}\psi_y = -\sum_{\langle xy\rangle} \cos(\theta_x - \theta_y - A_{xy}), \quad (1)$$

where $\psi_x \equiv e^{i\theta_x}$, $U_{xy} \equiv e^{iA_{xy}}$, and the sum runs over the bonds $\langle xy \rangle$ of a square lattice. The phases A_{xy} are uncorrelated quenched random variables with zero average. In most studies they are distributed with Gaussian probability

$$P_{\rm G}(A_{xy}) \propto \exp\left(-\frac{A_{xy}^2}{2\sigma}\right). \tag{2}$$

We denote the RP XY model with distribution (2) by GRP XY. We also consider the RP XY model with distribution (the cosine model)

$$P_{\rm C}(A_{xy}) \propto \exp\left(\frac{\cos A_{xy}}{\sigma}\right), \tag{3}$$

which we denote by CRP XY. Such a model is particularly interesting because the distribution (3) allows some exact calculations along the so-called Nishimori (N) line $T \equiv 1/\beta = \sigma$ [8, 9]. In both GRP XY and CRP XY models the pure XY model is recovered in the limit $\sigma \to 0$, while the so-called gauge-glass model [10] with uniformly distributed phase shifts is obtained in the limit $\sigma \to \infty$.

The nature of the different phases arising when varying the temperature T and the disorder parameter σ and the critical behavior at the phase transitions have been investigated in many theoretical and experimental works [1]–[56]. In spite of that, a conclusive picture of the phase diagram and of the critical behaviors has not been achieved yet.

The expected T–σ phase diagram for the GRP XY and CRP XY models, which is sketched in figure 1, presents two finite-temperature phases: a paramagnetic phase and a low-temperature phase characterized by quasi-long-range order (QLRO) for sufficiently small values of σ; see, e.g., [55] and references therein. The paramagnetic phase is separated from the QLRO phase by a transition line, which starts from the pure XY point (denoted by P in figure 1) at ($\sigma = 0, T = T_{XY} \approx 0.893$) and ends at a zero-temperature disorder-induced transition denoted by D at $(\sigma_{\rm D}, T = 0)$. The QLRO phase extends up to a maximum value $\sigma_{\rm M}$ of the disorder parameter, which is related to the point M $\equiv (\sigma_{\rm M}, T_{\rm M})$, where the tangent to the transition line is parallel to the T axis. No long-range glassy order can exist at finite temperature for any value of σ, including the gauge-glass limit $\sigma \to \infty$ [21, 22]. Several numerical studies of the gauge-glass XY model [5, 19, 36, 43, 45, 46], [49]–[51] support a zero-temperature glassy transition. A more complete discussion of the known features of the phase diagram will be reported below.

In this paper we investigate several controversial issues concerning the critical behavior at the magnetic and glassy transitions in RP XY models. In particular, we will check whether the critical behavior along the paramagnetic–QLRO transition line is universal and belongs to the universality class of the pure XY model, whether there is a multicritical point along the paramagnetic–QLRO transition line, and, finally, whether the $T = 0$ glassy transition extends from $\sigma = \infty$ to $\sigma_{\rm D}$ (see figure 1) and belongs to the same universality class as that in the XY gauge-glass model. For this purpose, we perform Monte Carlo (MC) simulations of the GRP XY and CRP XY models for several values of the temperature and of the variance σ, approaching the magnetic and glassy transition lines from the paramagnetic phase. As we shall see, our results for the CRP XY model provide robust evidence for a universal Kosterlitz–Thouless (KT) behavior of the magnetic correlations along the paramagnetic–QLRO transition line from the pure

J. Stat. Mech. (2010) P03006

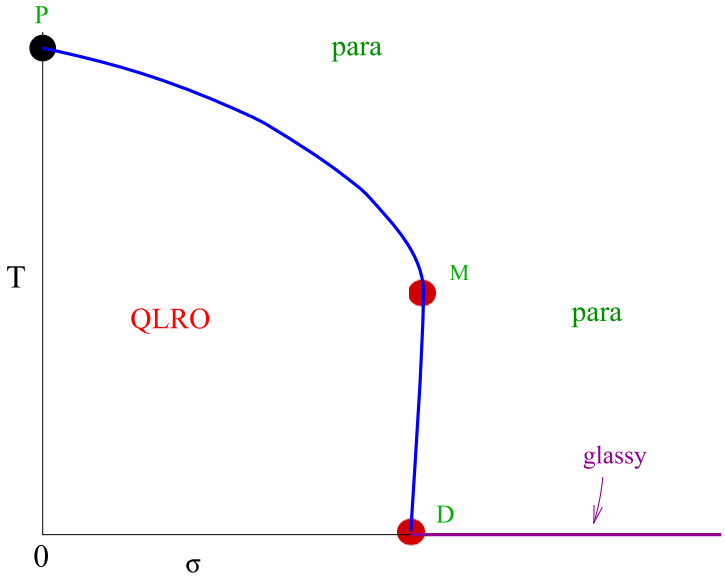

Figure 1. Phase diagram of RP XY models as a function of T and of the disorder distribution variance σ.

XY point P to the point M where the transition line runs parallel to the T axis and magnetic and overlap correlations are equal. Along the line the magnetic correlation length ξ behaves as $\ln \xi \sim u_{\rm t}^{-1/2}$, where $u_{\rm t}$ is the thermal scaling field, and the magnetic susceptibility as $\chi \sim \xi^{7/4}$ (corresponding to $\eta = 1/4$). On the other hand, the behavior of the overlap correlations appears to be σ dependent along this transition line. Moreover, the numerical results for the CRP XY model indicate that the point M is multicritical. We conjecture that these conclusions hold for any RP XY model. In all cases we expect the paramagnetic–QLRO transition line to be divided into two parts by a multicritical point M, where magnetic and overlap correlations have the same critical behavior, though they are not equal. At variance with what happens in the CRP XY model, the point M is not expected to coincide with the point at which the tangent to the transition line is parallel to the T axis: this coincidence should be a unique feature of the CRP XY model. Then, from P to M we expect any RP XY model to behave as the CRP XY, that is, showing a KT behavior for magnetic correlations and a σ dependent behavior for disorder-related quantities. The universality of the behavior has been confirmed by our numerical results for the GRP XY model.

Finally, we have investigated the critical behavior for large values of σ. Our numerical results provide strong evidence for a universal zero-temperature glassy transition for $\sigma > \sigma_{\rm D}$. For $T \to 0$ overlap correlation functions are critical, and, in particular, the corresponding correlation length $\xi_{\rm o}$ diverges as $\xi_{\rm o} \sim T^{-\nu}$ when $T \to 0$ with $\nu = 2.5(1)$.

This paper is organized as follows. In section 2 we review the known results for the phase diagram and for the critical behavior of the RP XY models. Section 3 provides the definitions of the quantities considered in our numerical work. In section 4 we study the critical behavior along the thermal paramagnetic–QLRO transition line which starts at the pure XY point P and ends at multicritical point M. In section 5 we discuss critical behavior along the N line of the CRP XY model and show that the point M where the N

doi:10.1088/1742-5468/2010/03/P03006

J. Stat. Mech. (2010) P03006

line intersects the critical line is multicritical. In section 6 we investigate the glassy critical behavior at $T = 0$ for $\sigma > \sigma_{\rm D}$. Finally, in section 7 we draw our conclusions. There are also several appendices. Appendix A reports some details of the MC simulations. Appendix B is devoted to a careful analysis of the KT renormalization-group (RG) equations and of the corresponding RG flow. We derive the most general form of the β function for the sine–Gordon model and discuss the structure of the scaling corrections in the XY model. These results are used in the discussion of the behavior at the paramagnetic–QLRO transition. In appendix C we discuss some features of the critical behavior at a multicritical point. In appendix D we briefly discuss the RG equations in the presence of randomness. Finally, in appendix E we report some analytical results for the magnetic correlations in the gauge-glass model.

2. The phase diagram

In figure 1 we show the expected T–σ phase diagram of the RP XY models. In the absence of disorder ($\sigma = 0$) the model shows a high-T paramagnetic phase and a low-T phase characterized by QLRO controlled by a line of Gaussian fixed points, where the spin–spin correlation function $\langle \bar\psi_x \psi_y \rangle$ decays as $1/r^{\eta(T)}$ for $r \equiv |x-y| \to \infty$, with η depending on T. The two phases are separated by a Kosterlitz–Thouless (KT) transition [57] at [58] $\beta_{XY} \equiv 1/T_{XY} = 1.1199(1)$. For $\tau \equiv T/T_{XY} - 1 \to 0^+$, the correlation length and the magnetic susceptibility diverge exponentially as $\ln \xi \sim \tau^{-1/2}$ and $\chi \sim \xi^{7/4}$, respectively. An interesting question is whether these features change in the presence of random phase shifts.

The low-temperature phase of RP XY models shows QLRO for sufficiently small values of σ. The universal features of the long-distance behavior are explained by the random-spin-wave theory [3], obtained by replacing

$$\cos(\theta_x - \theta_y - A_{xy}) \longrightarrow 1 - \tfrac{1}{2}(\theta_x - \theta_y + A_{xy})^2 \tag{4}$$

in Hamiltonian (1). This scenario has been accurately verified using Monte Carlo (MC) simulations in both GRP XY and CRP XY models [55]. The QLRO phase disappears for large values of σ (see, e.g., [6] and references therein); more precisely, as we shall see, for $\sigma \gtrsim 0.31$ in the case of the CRP XY model.

For $\sigma \to \infty$ phases are uniformly distributed and one obtains the gauge-glass model. Although this model has been much investigated [5, 10], [14]–[19], [21, 22, 25, 26, 29], [32]–[34], [36, 38, 40, 41], [43]–[52], [54], its phase diagram and critical behavior are still controversial. No long-range glassy order can exist at finite temperature [21, 22]. However, this does not exclude the possibility of more exotic low-temperature glassy phases [40, 47], for example a phase characterized by glassy QLRO. Many numerical works at finite and zero temperature support a zero-temperature transition [5, 19, 36, 43, 45, 46], [49]–[51]. According to this scenario, the correlation length determined from the overlap correlation function diverges as $\xi_{\rm o} \sim T^{-\nu}$ when approaching the critical point $T = 0$. The critical exponent ν has been estimated using finite-temperature Monte Carlo (MC) simulations; the findings were [45] $1/\nu = 0.39(3)$ and [49] $1/\nu = 0.36(3)$. The exponent ν is related to the $T = 0$ stiffness exponent θ by $\theta = -1/\nu$. The $T = 0$ numerical calculations of [43] and [51] provided the estimates $\theta = -0.36(1)$ and $\theta \approx -0.45$ respectively, which are consistent with the finite-temperature estimates of ν. The $T = 0$ transition scenario

J. Stat. Mech. (2010) P03006

has been questioned in [40, 41, 44, 47, 48], [52]–[54], which provide some numerical and experimental (for Josephson junction arrays with positional disorder [53]) evidence for the existence of a finite-temperature transition at $T \approx 0.2$, with a low-temperature glassy phase characterized by frozen vortices and glassy QLRO.

Other features of the phase diagram are better discussed within the CRP XY model, characterized by the random-phase-shift distribution (3), because of the existence of exact results along the so-called Nishimori (N) line [8, 9]

$$T \equiv 1/\beta = \sigma. \tag{5}$$

Along the N line the energy density E is known exactly:

$$E \equiv \frac{1}{V}[\langle \mathcal{H} \rangle] = -2\frac{I_1(\beta)}{I_0(\beta)}, \tag{6}$$

where $I_0(\beta)$ and $I_1(\beta)$ are modified Bessel functions. Moreover, the spin–spin and overlap correlation functions are equal:

$$[\langle \bar{\psi}_x \psi_y \rangle] = [|\langle \bar{\psi}_x \psi_y \rangle|^2]. \tag{7}$$

As already noted in [9], the N line should play an important role in the phase diagram, because it is expected to mark the crossover between the magnetism-dominated region and the disorder-dominated one.

In the GRP XY and CRP XY models, the paramagnetic phase is separated from the magnetic QLRO phase by a transition line, which starts from the pure XY point (denoted by P in figure 1) at ($\sigma = 0, T = T_{XY} \approx 0.893$) and ends at a $T = 0$ transition point induced by disorder (denoted by D) at ($\sigma_{\rm D}, T = 0$), where $\sigma_{\rm D} > 0$.[4] An important result has been proven for the CRP XY model [8]: the critical value $\sigma_{\rm M}$ of σ along the N line is an upper bound for the values of σ where magnetic QLRO can exist. Therefore, at the critical point M $\equiv (\sigma_{\rm M}, T_{\rm M})$, the tangent to the critical line should be parallel to the T axis; moreover, the critical value $\sigma_{\rm D}$ at $T = 0$ must satisfy $\sigma_{\rm D} \leq \sigma_{\rm M}$.

It is worth noting how similar the phase diagrams of the CRP XY model and of the square-lattice $\pm J$ Ising model in the T–p plane are; see figures 1 and 2, respectively. The square-lattice $\pm J$ (Edwards–Anderson) Ising model is defined by the Hamiltonian

$$\mathcal{H}_{\pm J} = -\sum_{\langle xy \rangle} J_{xy}\sigma_x\sigma_y, \tag{8}$$

where $\sigma_x = \pm 1$, the sum is over pairs of nearest-neighbor sites of a square lattice, and J_{xy} are uncorrelated quenched random variables, taking values $\pm J$ with probability distribution $P(J_{xy}) = p\delta(J_{xy} - J) + (1-p)\delta(J_{xy} + J)$. This model presents an analogous N line [59] in the T–p phase diagram, defined by $\tanh(1/T) - 2p + 1 = 0$. The transition point along the N line is a multicritical point (MNP) [60, 61]. Moreover, the critical behaviors for $T > T_{\rm MNP}$ and $T < T_{\rm MNP}$ are different. From the pure Ising point at $p = 1$ to the MNP the critical behavior is analogous to that observed in 2D randomly dilute Ising (RDI) models [62]. From the MNP to the $T = 0$ axis the critical behavior belongs

[4] We mention that the first renormalization-group (RG) analyses based on a Coulomb-gas description [3] predicted $\sigma_{\rm D} = 0$, but it was later clarified that this was an artifact of the approximations. Indeed, experimental [11] and numerical works [11]–[13], [30], as well as refinings of the RG arguments [8, 23, 27, 28, 31, 35], have shown the absence of a re-entrant transition for sufficiently small values of σ.

J. Stat. Mech. (2010) P03006

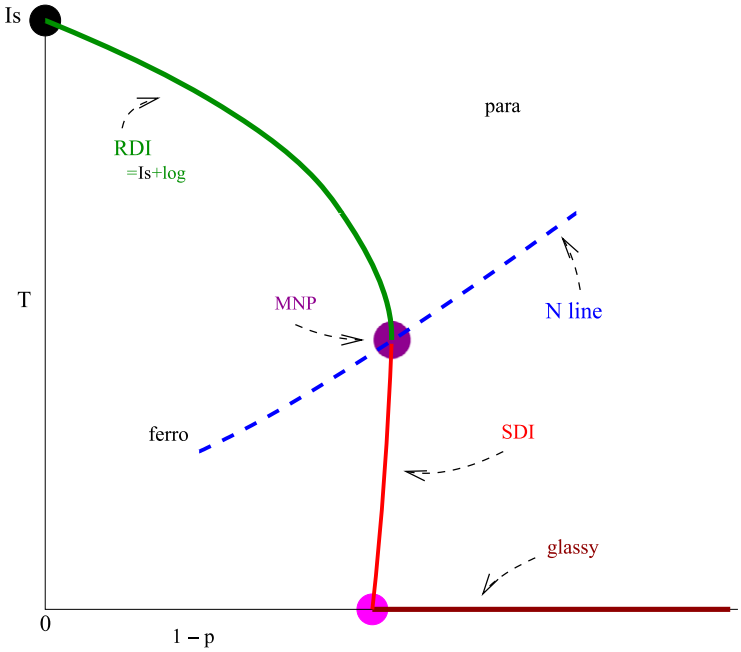

Figure 2. Phase diagram of the $\pm J$ (Edwards–Anderson) Ising model on the square lattice. The phase diagram is symmetric under $p \to 1-p$.

to a new strong-disorder Ising (SDI) universality class [63]. Finally, the $T = 0$ endpoint of the low-temperature paramagnetic–ferromagnetic transition line is the starting point of a $T = 0$ transition line, characterized by a glassy universal critical behavior [64].

In [8] it was also argued that, in the RP XY models (in particular, in the CRP XY one) the low-temperature paramagnetic–QLRO transition line from the critical point M to the point D runs parallel to the T axis, and so $\sigma_{\rm D} = \sigma_{\rm M}$. The same arguments fail in the 2D $\pm J$ Ising model [60, 61, 63, 65, 66], although they provide a good approximation. Thus, they are likely not exact also in the case of the RP XY models, although they may still provide a good approximation, suggesting that $0 < \sigma_{\rm M} - \sigma_{\rm D} \ll \sigma_{\rm M}$.

In the phase diagram reported in figure 1, which refers to the CRP XY, we may distinguish two transition lines meeting at point M: the thermal paramagnetic–QLRO transition line from P to M, which can be approached by decreasing the temperature at fixed σ, and the transition line from M to D, which can be instead observed by changing the disorder at fixed T for sufficiently low temperatures. As we shall see, our numerical results for the CRP XY model provide some evidence that the point M is multicritical. We conjecture that the same conclusion holds for generic RP XY models, though in the generic case we do not expect the multicritical point M to coincide with the point where the tangent to the critical line is parallel to the T axis.

The phase transition from the paramagnetic to the QLRO phase is generally expected to be of KT type ($\ln \xi$ is expected to have a power-law divergence), but its specific features, for instance the precise form of the power-law behavior and the value of the exponent η, have not been conclusively determined yet. Some numerical results supporting the KT-like behavior were presented in [30]. The disorder-driven $T = 0$ transition at $\sigma_{\rm D}$ has been argued [23, 24, 30, 35, 42] to show a KT-like behavior with $\ln \xi \sim (\sigma - \sigma_{\rm D})^{-1}$ and

$\chi \sim \xi^{2-\eta}$ with $\eta = 1/16$. However, other RG studies [28, 31] obtained a different behavior: $\ln \xi \sim (\sigma - \sigma_{\rm D})^{-1/2}$. The value of η associated with the magnetic two-point function has been believed to vary along the critical line [3, 23, 28, 31], from $\eta = 1/4$ for the pure XY model at $\sigma = 0$ to $\eta = 1/16$ at the $T = 0$ transition. As we shall see, our numerical results along the thermal paramagnetic–QLRO transition line, from P to and including M, strongly support $\eta = 1/4$, independently of σ.

In the following sections we investigate some of the open issues of the RP XY models, by performing MC simulations of the GRP XY and CRP XY models close to their magnetic and glassy transition lines. In particular, we investigate the critical behavior at the thermal paramagnetic–QLRO transition line (from point P to the multicritical point), along the N line in the CRP XY model, and at the $T = 0$ glassy transition line for large disorder.

3. Notation

We consider RP XY models defined on square lattices of size L^2 with periodic boundary conditions. We define the magnetic spin–spin correlation function

$$G(x-y) \equiv [\langle \bar{\psi}_x \, \psi_y \rangle] \tag{9}$$

and the overlap correlation function

$$G_{\rm o}(x-y) \equiv [|\langle \bar{\psi}_x \, \psi_y \rangle|^2]. \tag{10}$$

The angular and square brackets indicate the thermal average and the quenched average over disorder, respectively. The latter can also be written in terms of the overlap variables. Given two copies of the system with spins $\psi_x^{(1)}$ and $\psi_x^{(2)}$, we define

$$q_x = \bar{\psi}_x^{(1)} \psi_x^{(2)}, \qquad G_{\rm o}(x-y) = [\langle \bar{q}_x \, q_y \rangle], \tag{11}$$

where the thermal average is performed over the two systems with the same disorder configuration. We define the magnetic susceptibility $\chi \equiv \sum_x G(x)$, the overlap susceptibility $\chi_{\rm o} \equiv \sum_x G_{\rm o}(x)$, and the second-moment correlation lengths

$$\xi^2 \equiv \frac{\tilde{G}(0) - \tilde{G}(q_{\rm min})}{\hat{q}^2_{\rm min} \tilde{G}(q_{\rm min})}, \qquad \xi^2_{\rm o} \equiv \frac{\tilde{G}_{\rm o}(0) - \tilde{G}_{\rm o}(q_{\rm min})}{\hat{q}^2_{\rm min} \tilde{G}_{\rm o}(q_{\rm min})}, \tag{12}$$

where $q_{\rm min} \equiv (2\pi/L, 0)$, $\hat{q} \equiv 2 \sin q/2$.

We also define the quartic couplings

$$g_4 \equiv -\frac{3\chi_4}{2\chi^2 \xi^2}, \qquad \chi_4 \equiv \frac{1}{V}[\langle |\mu|^4 \rangle - 2\langle |\mu|^2 \rangle^2], \tag{13}$$

$$g_{22} \equiv -\frac{\chi_{22}}{\chi^2 \xi^2}, \qquad \chi_{22} \equiv \frac{1}{V}\left([\langle |\mu|^2 \rangle^2] - [\langle |\mu|^2 \rangle]^2 \right), \tag{14}$$

$$g_{\rm c} \equiv g_4 + 3 g_{22}, \tag{15}$$

where $\mu \equiv \sum_x \psi_x$ and $V = L^2$. Note that for the pure XY model, $g_{22} = 0$ and $g_{\rm c} = g_4$. Finally, we define an overlap quartic coupling $g_{\rm o}$ as

$$g_{\rm o} \equiv -\frac{3\bar{\chi}_{4{\rm o}}}{2\chi_{\rm o}^2 \xi_{\rm o}^2}, \qquad \bar{\chi}_{4{\rm o}} = \frac{1}{V}[\langle |\mu_{\rm o}|^4 \rangle] - 2[\langle |\mu_{\rm o}|^2 \rangle]^2, \tag{16}$$

where $\mu_{\rm o} \equiv \sum_x q_x$.

J. Stat. Mech. (2010) P03006

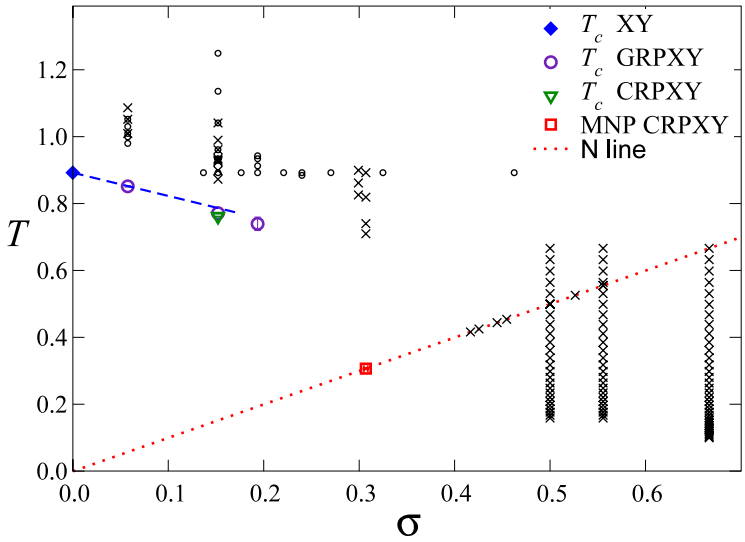

Figure 3. Values of $T \equiv 1/\beta$ and σ where MC data were collected. The circles and crosses refer to the GRP XY and CRP XY models, respectively. The dotted line $T = \sigma$ is the N line for the CRP XY model. We also show some estimates of T_c for the GRP XY and CRP XY models, and the critical point (MNP) of the CRP XY model along the N line. The dashed line is the prediction (27) for the behavior of T_c at small values of σ.

4. Critical behavior along the thermal paramagnetic–QLRO transition line

In this section we study the critical behavior of the RP XY models along the thermal paramagnetic–QLRO transition line (see figure 1), which starts at the point P on the $\sigma = 0$ axis and ends at the multicritical point, which belongs to the N line in the CRP XY model. For this purpose, we perform MC simulations of the GRP XY and of the CRP XY model for several values of T and σ in the paramagnetic phase, where the magnetic correlation length ξ is large but finite. Figure 3 shows the points where the simulations are performed. The MC algorithm is described in appendix A. We average over a large number of samples, $N_s \approx 10^4$ in most cases. We consider large lattice sizes, satisfying $L/\xi \gtrsim 10$, in order to make finite-size effects negligible and obtain infinite-volume results. The residual finite-size effects are in all cases smaller than, or at most comparable with, the statistical errors.

In the following we first discuss the critical behavior of the magnetic spin–spin correlation function (9). We show that disorder is apparently irrelevant: for any σ the correlation length diverges following the KT law valid for $\sigma = 0$ and the magnetic susceptibility diverges with critical exponent η equal to 1/4. Then, we discuss the behavior of observables related to the overlap correlation function (10), finding that the critical behavior of these quantities is apparently σ dependent.

4.1. Critical behavior approaching the pure XY transition point

We wish now to understand the critical behavior along any line that lies in the paramagnetic phase and ends at the pure XY critical point at $\sigma = 0$ and $T = T_{XY}$.

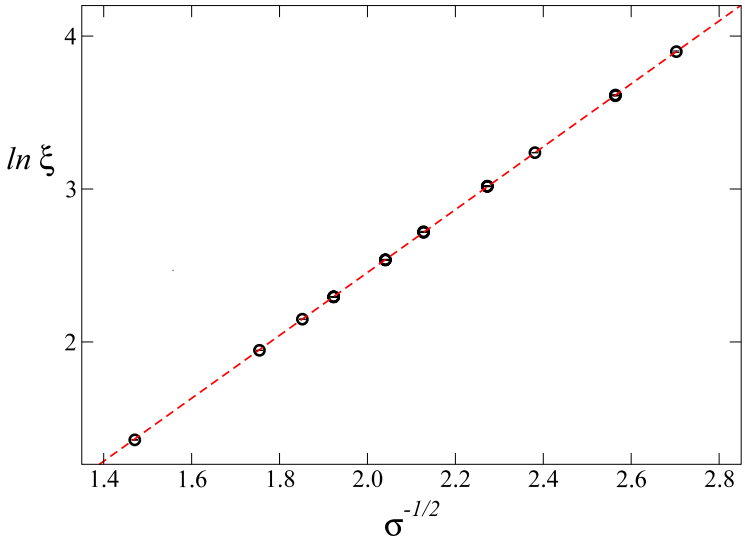

Figure 4. MC estimates of ξ for $\beta = \beta_{XY} = 1.1199$ and several values of σ versus $\sigma^{-1/2}$. The dashed line corresponds to a linear fit to $\ln \xi = C_\sigma \sigma^{-1/2} + b$.

For $\sigma = 0$, as T approaches the critical temperature T_{XY} from above (the paramagnetic phase), the magnetic correlation length ξ diverges as

$$\ln(\xi/X) = C\tau^{-1/2} + \mathrm{O}(\tau^{1/2}), \qquad \tau \equiv (T - T_{XY})/T_{XY}, \tag{17}$$

where X and C are nonuniversal constants. In the case of the square-lattice XY model with nearest-neighbor interactions [58] $\beta_{XY} \equiv 1/T_{XY} = 1.1199(1)$, $X = 0.233(3)$ and $C = 1.776(4)$.[5] The magnetic susceptibility χ diverges as (see appendix B)

$$\chi = A_\chi \xi^{7/4} \left[1 + \frac{b_\chi}{\ln(\xi/X)} + \mathrm{O}\left(1/\ln^2 \xi\right) \right]. \tag{18}$$

Note that while A_χ is a nonuniversal amplitude, the coefficient b_χ of the leading logarithmic corrections is universal. As shown in appendix B, it can be computed from the perturbative expansion of the RG dimension of the spin variable; the result is $b_\chi = \pi^2/16$.

We now consider the GRP XY model and study the critical behavior of χ and ξ as one approaches the pure XY critical point along the line $\beta = \beta_{XY} = 1.1199$ by decreasing σ. We collected data for $0.46 \gtrsim \sigma \gtrsim 0.14$ in the infinite-volume limit, corresponding to the quite large range of correlation lengths $4 \lesssim \xi \lesssim 50$. Figure 4 shows a plot of $\ln \xi$ versus $\sigma^{-1/2}$. The data fall on a straight line, showing that for $\sigma \to 0$

$$\ln \xi \sim \sigma^{-1/2}. \tag{19}$$

This behavior can be understood within the RG framework. The general discussion presented in appendix C shows that, as long as disorder is less relevant than the thermal

[5] Equation (17) holds whatever the definition of the correlation length is, but of course X depends on the specific choice for ξ. Reference [58] studied the exponential correlation length ξ_{gap}, which is defined as the inverse of the mass gap, and determined the corresponding constant $X_{\mathrm{gap}} = 0.233(3)$. Since in the critical limit [67] $\xi^2/\xi^2_{\mathrm{gap}} = r = 0.9985(5)$, the constant X for the second-moment correlation length that we use is given by $X = X_{\mathrm{gap}}\sqrt{r} = 0.233(3)$.

J. Stat. Mech. (2010) P03006

perturbation, the critical behavior can be simply obtained by replacing τ with the nonlinear thermal scaling field. Note that it is not necessary that disorder is irrelevant to obtain the result (19). In general, the thermal nonlinear scaling field $u_{\rm t}$ is an analytic function of the system parameters. Thus, in the presence of disorder it is a function of both $\tau = (T - T_{XY})/T_{XY}$ and σ such that, close to the XY transition point, it behaves as

$$u_{\rm t}(\tau, \sigma) = \tau + c_\sigma \sigma + \cdots \tag{20}$$

where the dots stand for higher-order terms. If disorder is less relevant than the thermal perturbation, then

$$\ln(\xi/X) = C u_{\rm t}^{-1/2} + {\rm O}(u_{\rm t}^{1/2}), \tag{21}$$

along any straight line in the T, σ plane which ends at the XY pure transition point. Since this relation also holds for $\sigma = 0$ and $u_{\rm t}(\tau, 0) = \tau$, C and X are the same constants as reported below (17). Along the line $T = T_{XY}$ equation (21) implies

$$\ln(\xi/X) = \frac{C}{(c_\sigma \sigma)^{1/2}} + {\rm O}(\sigma^{1/2}), \tag{22}$$

in agreement with the observed behavior. In order to determine c_σ we have performed fits to

$$\ln(\xi/X) = C_\sigma \sigma^{-1/2} \left(1 + b\sigma\right), \tag{23}$$

using $X = 0.233(3)$. We obtain the estimates $C_\sigma = 2.010(2)$ and $b \approx -0.11$. In particular, a fit of the data satisfying $\xi \gtrsim 7$ gives $C_\sigma = 2.0102(8)$ and $b = -0.108(2)$, with $\chi^2/{\rm DOF} \approx 1.1$ (DOF is the number of degrees of freedom of the fit). Using $C = 1.776(4)$ and $C_\sigma = C/\sqrt{c_\sigma}$, we obtain

$$c_\sigma = \left(\frac{C}{C_\sigma}\right)^2 = 0.781(4). \tag{24}$$

The constant c_σ is nonuniversal and as such is model dependent. However, for $\sigma \to 0$ the fields A_{xy} are typically very small and the distribution functions for the GRP XY and CRP XY models are identical to leading order in A_{xy}. We thus expect the first corrections to the thermal scaling field due to disorder to be identical in the two models, i.e.

$$u_{\rm t,GRP}{}_{XY}(\tau, \sigma) = u_{\rm t,CRP}{}_{XY}(\tau, \sigma) + {\rm O}(\sigma^2), \tag{25}$$

which implies that c_σ is the same in the GRP XY and CRP XY models.

4.2. Critical behavior of the magnetic correlations at fixed σ

Standard arguments that apply to critical lines and multicritical points imply that the critical temperature at fixed σ must be the solution of the equation

$$u_{\rm t}[T_{\rm c}(\sigma), \sigma] = 0. \tag{26}$$

Therefore, equation (20) also implies that for small values of σ the critical temperature for the GRP XY model (and also for the CRP XY model if (25) holds) is given by

$$T_{\rm c}(\sigma) = T_{XY}[1 - c_\sigma \sigma + {\rm O}(\sigma^2)]. \tag{27}$$

J. Stat. Mech. (2010) P03006

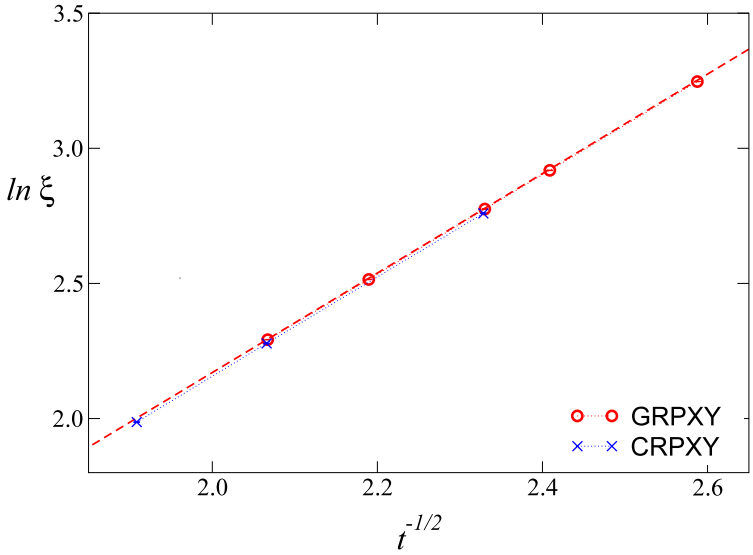

Figure 5. Plots of $\ln\xi$ versus $t^{-1/2}$, where $t \equiv (T - T_c)/T_c$, for the GRP XY and CRP XY models at $\sigma = 0.0576$. For both models we use $T_c = 0.8528$, as obtained by using (27). The dashed line corresponds to a fit of the GRP XY data to $\ln\xi = ct^{-1/2} + a$. The dotted line that connects the MC data is drawn to guide the eye.

Equation (27) can be checked by analyzing data at fixed small values of σ. We have performed MC simulations of the GRP XY model at $\sigma = 0.0576$ for several values of β, from $\beta = 0.95$ to 1.02, corresponding to $10 \lesssim \xi \lesssim 26$, and of the CRP XY model at the same value of σ for $\beta = 0.92, 0.95, 0.99$ corresponding to $7 \lesssim \xi \lesssim 16$. In figure 5 we plot ξ versus $t^{-1/2}$ with $t \equiv T/T_c - 1$ and $T_c = 0.8528$ given by (27) (if we take the errors on T_{XY} and c_σ into account, we have $T_c = 0.8528(3)$). Clearly, $\xi \to \infty$ as $t \to 0$, confirming (27). Moreover, it is clearly consistent with the KT behavior

$$\ln\xi = at^{-1/2} + b. \tag{28}$$

A fit of all available data for the GRP XY model to (28) gives $a = 1.841(2)$ and $b = -1.511(5)$ (with $\chi^2/\mathrm{DOF} \approx 1.3$) keeping $T_c = 0.8528$ fixed. A nonlinear fit, taking T_c as a free parameter, gives $T_c = 0.852(2)$, in good agreement with (27). Note that the estimate of the constant b is close to the corresponding XY model value $\ln X = -1.46(1)$. This is not unexpected since $X(\sigma) = X + \mathrm{O}(\sigma)$.

We also collected data at $\sigma = 0.1521$ for both the GRP XY and CRP XY models, for $0.8 \le \beta \le 1.1199$ (corresponding to $2 \lesssim \xi \lesssim 37$) and $0.96 \le \beta \le 1.145$ (corresponding to $5 \lesssim \xi \lesssim 46$), respectively. Again, the data fit well to the KT behavior (28); see figure 6. Fits of the MC data for $\xi \gtrsim 10$ to (28) (for which $\chi^2/\mathrm{DOF} < 1$) give the estimates $T_c = 0.772(2)$ for the GRP XY model, and $T_c = 0.762(1)$ for the CRP XY model. Note that (27) would give $T_c = 0.7872$ for $\sigma = 0.1521$, which is slightly larger than the above estimates. This is not unexpected since, when increasing σ, higher-order terms (which are different for the two models) may become important in (20). We also mention the estimates $b = -1.82(7)$ and $b = -1.78(3)$ for the GRP XY and CRP XY models, respectively, from which one obtains estimates of the corresponding length scale

J. Stat. Mech. (2010) P03006

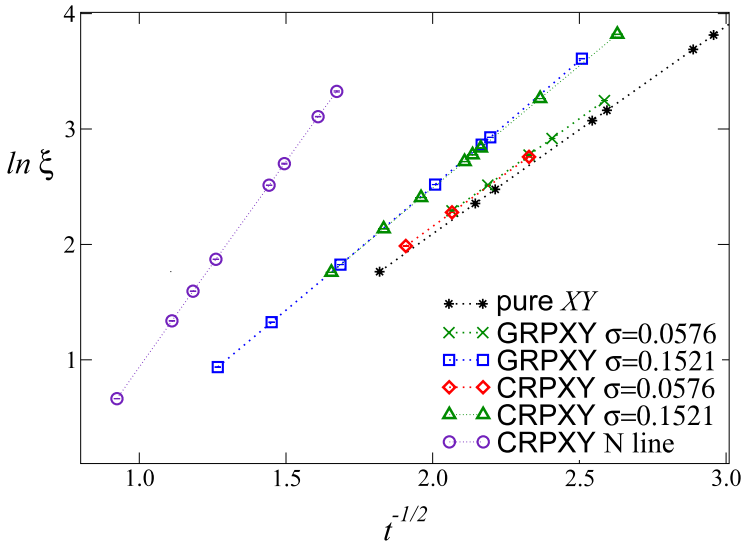

Figure 6. Estimates of $\ln \xi$ versus $t^{-1/2}$, where $t \equiv T/T_c(\sigma) - 1$, for the GRP XY and CRP XY models for several values of σ. For $\sigma = 0.0576$ we take $T_c(\sigma) = 0.8528$ (equation (27)). For the other values of σ, $T_c(\sigma)$ is determined from the data. The lines are drawn to guide the eye. The data for the XY case are taken from [68].

$X(\sigma) = e^b$, $X = 0.162(11)$ and $X = 0.169(5)$. We also determined ξ for other values of σ, but in a smaller range. The results are compatible with a KT behavior, but they do not allow us to get robust estimates of T_c. We only mention that in the case of the GRP XY at $\sigma = 0.1936$, for which we have only data for $\xi \lesssim 20$, we find $T_c \approx 0.74$.

At a KT transition the magnetic susceptibility behaves as in (18), where $b_\chi = \pi^2/16$ is universal. In figure 7 we show $\chi/\xi^{7/4}$ for GRP XY and CRP XY and several values of σ together with those for the pure XY model taken from [68]. We report the data versus $\ln \xi/X(\sigma = 0)$. We could also have used $\ln \xi/X(\sigma)$, where $X(\sigma)$ is determined from the fit of ξ. This choice gives a plot essentially identical to the one reported, which is not unexpected since, by using $\ln \xi/X(\sigma = 0)$ or $\ln \xi/X(\sigma)$ one simply changes the corrections of order $\sigma/\ln^2 \xi/X$, which are present anyway. The results appear to follow the same curve within the errors (except those obtained along the N line, which we shall discuss in section 5). They provide strong evidence that the value $\eta = 1/4$ is universal along the thermal paramagnetic–QLRO transition line. Also the slope appears universal (the coefficient b_χ does not depend on σ), as expected on the basis of the discussion of appendix B. The constant A_χ corresponds to the intercept of $\chi/\xi^{7/4}$ at $1/\ln \xi/X(\sigma) = 0$. As can be seen from the figure, this constant, which is not universal, varies very little with σ: differences are not visible within our errors, except for the CRP XY data at $\sigma = 0.307$. However, note that for this value of σ the critical behavior is controlled by the multicritical Nishimori point, i.e. by the special point M which appears in figure 1; we will return to this in section 5.

In conclusion, the above numerical results provide strong evidence that the magnetic two-point correlations show a KT behavior along the thermal paramagnetic–QLRO transition line in GRP XY and CRP XY models.

J. Stat. Mech. (2010) P03006

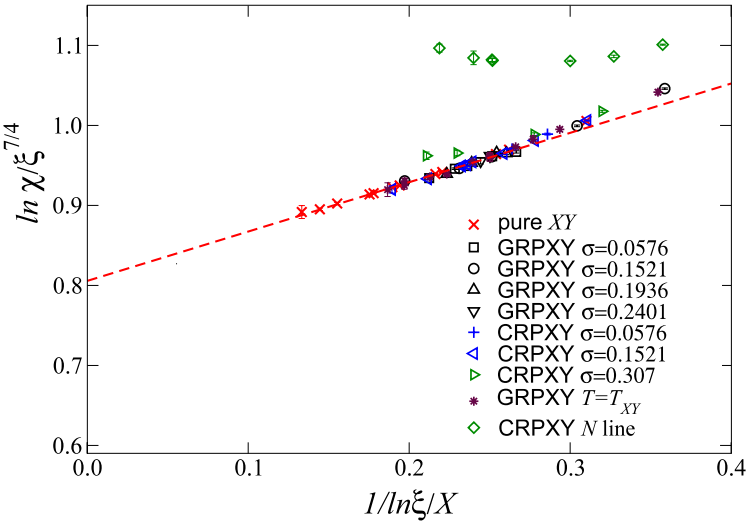

Figure 7. Plot of $\ln(\chi/\xi^{7/4})$ versus $1/\ln\xi/X$. We fix $X = 0.233$, which is the length scale value valid for the pure XY model. We show data for the pure XY model (taken from [68]), and for the GRP XY and CRP XY models at various values of σ, at $T = T_{XY}$ and along the N line. The dashed line corresponds to a fit to $a + \pi^2/(16\ln\xi/X)$ of the pure XY data satisfying $\xi \gtrsim 10$ (we obtain $a = 0.8058(1)$ with $\chi^2/\mathrm{DOF} \approx 0.7$).

4.3. Quartic couplings

We now discuss the behavior of the quartic couplings defined in (13)–(15). We recall that in the pure XY model $g_{22} = 0$ while $g_4 = g_c$ behaves as

$$g_4 = g_4^* + \frac{b_g}{(\ln\xi/X)^2} + \mathrm{O}(1/\ln^4\xi), \tag{29}$$

where g_4^* and b_g are universal; see appendix B. We mention the estimates $g_4^* = 13.65(6)$ obtained by form-factor computations in [68], and $g_4^* = 13.7(2)$ by field-theoretical methods [69]; other results for g_4^* can be found in [70] and references therein.

In figure 8 we show some MC results for g_c for the CRP XY model at $\sigma = 0.1521, 0.0576$ and the GRP XY model at $\beta = \beta_{XY} = 1.1199$ (within our errors of a few per mille the infinite-volume limit is reached for $L/\xi \gtrsim 10$, as in the pure XY model [68]), and compare them with MC results for the pure XY model taken from [68]. The results are identical within errors. For example, if we consider the CRP XY model for $\sigma = 0.1521$, a fit to $g_c^* + b_g/(\ln\xi/X)^2$ gives $g_c^* = 13.57(10)$ and $b_g = -3.1(1.4)$, with $\chi^2/\mathrm{DOF} \approx 0.4$, to be compared with the value [68] $g_4^* = 13.65(6)$ of the pure XY model. Both g_c^* and b_g, which are universal in the pure XY universality class, do not depend on σ.

The quartic coupling g_{22} defined in (14) is interesting because it is particularly sensitive to randomness effects, since in the pure XY model it vanishes trivially. The estimates of g_{22} in the GRP XY model for $T = T_{XY}$ and several values of σ are shown in figure 9. They decrease with decreasing σ, and appear to vanish when $\sigma \to 0$ as

$$g_{22} \sim c\xi^{-\varepsilon}, \tag{30}$$

J. Stat. Mech. (2010) P03006

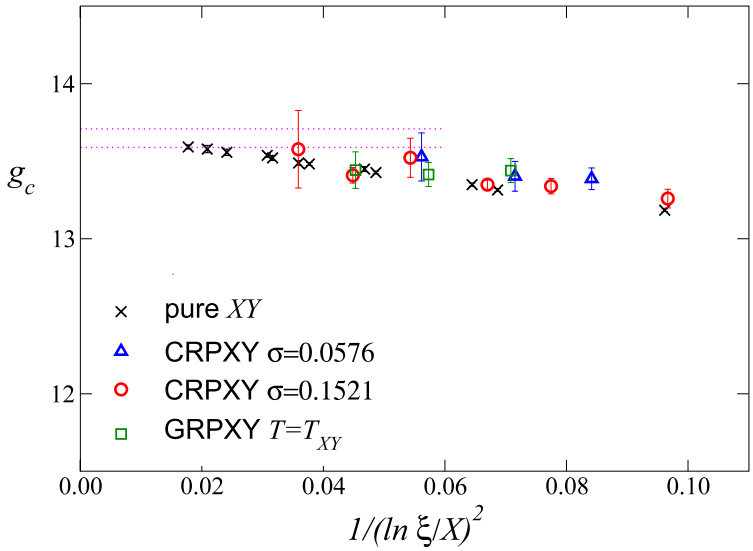

Figure 8. MC estimates of $g_c \equiv g_4 + 3g_{22}$ versus $1/(\ln \xi/X)^2$ with $X = 0.233$. The data for the pure XY model are taken from [68]. The dotted lines correspond to the estimate $g_c^* = g_4^* = 13.65(6)$ obtained by form-factor calculations [68].

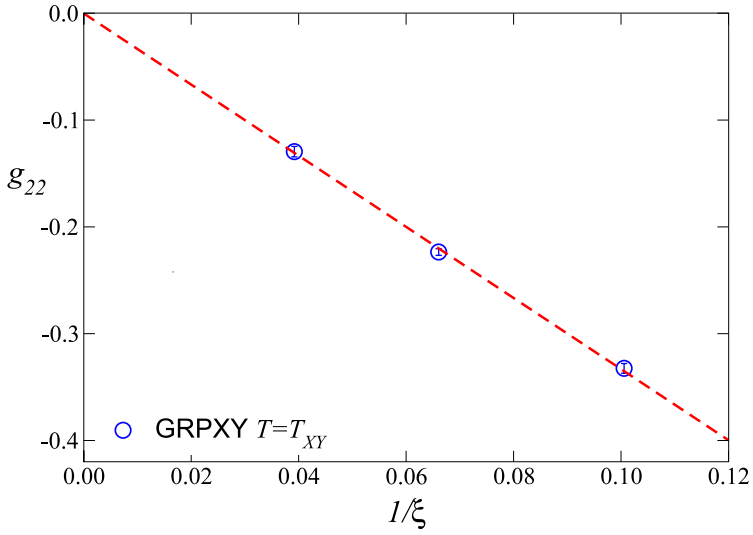

Figure 9. Estimates of g_{22} versus $1/\xi$ for the GRP XY model at fixed $\beta = \beta_{XY} = 1.1199$. The line is a fit of g_{22} to $c\xi^{-1}$.

with $\varepsilon \approx 1.0$. A fit to (30) gives $\varepsilon = 0.97(4)$, $c = 3.1(3)$ with $\chi^2/\mathrm{DOF} \approx 1.1$, where DOF is the number of degrees of freedom of the fit.

The fast decrease of g_{22} along the line $T = T_{XY}$ (note that $g_{22} \sim 1/\xi$ implies $g_{22} \sim \exp(-c\sigma^{-1/2})$) might suggest irrelevance of the disorder, and therefore that the critical value g_{22}^* vanishes along the thermal paramagnetic–QLRO transition line. This conclusion is apparently contradicted by the results at fixed $\sigma > 0$. The results for the CRP XY model at various values of σ, $\sigma = 0.0576, 0.1521, 0.2992, 0.307$, are shown in figure 10, where they are plotted versus $(\ln \xi/X)^{-2}$, which is the correction expected in

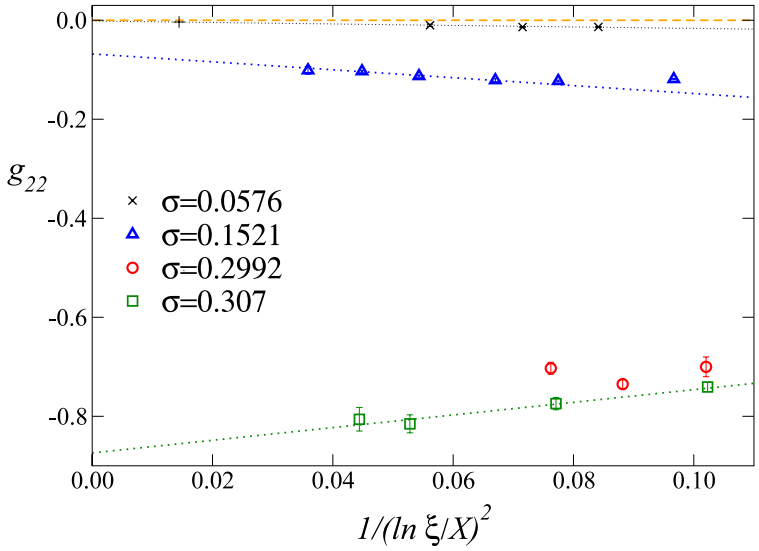

Figure 10. Estimates of g_{22} for the CRP XY model at various values of σ. The lines show linear extrapolations to the critical point. A data point denoted by a plus along the line related to $\sigma = 0.0576$ is obtained by using (30) and (23) with the results of the fits along the $T = T_{XY}$ line.

the pure XY model for RG invariant quantities. The coupling g_{22} is quite small, but definitely different from zero on the transition line. For $\sigma = 0.1521$ an extrapolation using $g_{22}^* + b/(\ln \xi/X)^2$ suggests a nonzero critical limit. Using only data satisfying $\xi \gtrsim 10$, this fit gives $g_{22}^* = -0.068(8)$ and $b = -0.080(15)$, with $\chi^2/\mathrm{DOF} \approx 0.4$. We should also mention that the data for the largest values of ξ, those satisfying $\xi \gtrsim 10$ say, may be consistent with a vanishing critical limit, but only assuming a slower logarithmic approach, i.e., $g_{22} \approx b/(\ln \xi/X)$. For instance, the data with $\xi \gtrsim 10$ are consistent with this behavior (the fit gives $b = -0.482(4)$ with $\chi^2/\mathrm{DOF} \approx 1.1$). At $\sigma = 0.0576$ the $1/(\ln \xi)^2$ extrapolation of the data satisfying $7 \lesssim \xi \lesssim 16$ gives $g_{22}^* = -0.008(6)$ with $\chi^2/\mathrm{DOF} \approx 1.3$. The data for g_{22} at $\sigma \approx 0.30$ are larger, but this can be explained by crossover effects, since this value of σ is quite close to the critical point along the N line, where the critical behavior may change; see section 5.

Overall the results for g_{22} suggest a nonuniversal critical value.

4.4. Critical behavior of the overlap correlations

We now discuss the critical behavior of overlap correlations (cf (11)), which are the appropriate quantities for understanding the role of disorder. We consider the critical behavior of the overlap susceptibility which is expected to behave as $\chi_{\mathrm{o}} \sim \xi_{\mathrm{o}}^{2-\eta_{\mathrm{o}}}$. In the case of the pure XY model we have $\eta_{\mathrm{o}} = 2\eta = 1/2$. In [55] it was noted that the following relations:

$$2\eta - \eta_{\mathrm{o}} \approx \frac{\sigma}{\pi} \qquad \text{for GRP}XY, \tag{31}$$

$$2\eta - \eta_{\mathrm{o}} \approx \frac{\sigma + (1/2)\sigma^2}{\pi} \qquad \text{for CRP}XY \tag{32}$$

hold approximately over the whole QLRO phase (within the small statistical errors), even very close to the KT transition, as long as σ is not to large (in practice σ should not be close to $\sigma_{\rm M}$, where M is the Nishimori point defined in figure 1). This would suggest that they may remain valid up to the transition. Given the strong numerical evidence that the exponent η associated with the magnetic correlation is $\eta = 1/4$ (see section 4.2), the above relations imply that $\eta_{\rm o}$ varies along the paramagnetic–QLRO transition line approximately as

$$\eta_{\rm o} \approx \frac{1}{2} - \frac{\sigma}{\pi} \qquad \text{for GRP}XY, \tag{33}$$

$$\eta_{\rm o} \approx \frac{1}{2} - \frac{\sigma + \sigma^2/2}{\pi} \qquad \text{for CRP}XY, \tag{34}$$

at least for sufficiently small values of σ. We wish now to establish whether the high-temperature data are consistent with these predictions. In figure 11 we plot $\chi_{\rm o}/\xi^{2-\eta_{\rm o}}$ versus $1/\ln(\xi/X)$. The scaling is reasonable. We also report $\chi_{\rm o}/\xi^{2-\eta_{\rm o}}$, fixing $\eta_{\rm o}$ to the pure XY value $\eta_{\rm o} = 1/2$. Again the ratio is consistent with a limiting finite value. However, if $\chi_{\rm o}$ behaves as in the pure XY model, we would expect a σ independent slope (see appendix B), which is not supported by the data.

We now consider the ratio $\xi_{\rm o}/\xi$ between the second-moment correlation lengths obtained from the overlap and spin correlation functions; cf (12).[6] In order to estimate this ratio in the case of the pure XY model, we performed MC simulations (using the cluster algorithm) in the range $0.93 \le \beta \le 1.033$ corresponding to $12 \lesssim \xi \lesssim 110$. Taking into account the logarithmic scaling corrections, i.e. fitting the XY model data satisfying $\xi \gtrsim 32$ to $a + b/(\ln \xi/X)^2$ with $X = 0.233$, we obtain the estimate $\xi_{\rm o}/\xi = 0.417(4)$. In figure 12 we show the results for several values of σ. They are all consistent with a finite critical value, confirming that the paramagnetic–QLRO transitions are characterized by a single diverging length. The results can be extrapolated by assuming $\xi_{\rm o}/\xi = a + b/(\ln \xi/X)^2$ for $\xi \to \infty$. We obtain $\xi_{\rm o}/\xi = 0.417(5), 0.428(5), 0.425(7), 0.425(3)$ for the GRP XY model at $\sigma = 0.0576, 0.1521, 0.1936$ and the CRP XY model at $\sigma = 0.1521$, respectively. A larger result is found for the CRP XY model at $\sigma \approx 0.299$, 0.307: $\xi_{\rm o}/\xi \approx 0.49$.

These results indicate that the ratio $\xi_{\rm o}/\xi$ varies along the transition line, although it changes very weakly for small values of σ. Again, this is consistent with the observation that disorder-related quantities, like $\eta_{\rm o}$ and g_{22}, depend on σ.

5. Critical behavior along the N line in the CRP XY model

We now consider the critical behavior along the N line $T = \sigma$ in the CRP XY model, approaching the transition point from the paramagnetic phase. We recall that along the N line the magnetic and overlap correlation functions are equal, so $\eta_{\rm o} = \eta$ and $\xi_{\rm o} = \xi$ exactly. We performed several MC simulations along the N line, in the range $1.5 \le \beta \le 2.4$, corresponding to $2 \lesssim \xi \lesssim 28$, and considered large lattice sizes, in order to obtain infinite-volume results.

[6] In a Gaussian theory without disorder, in which the magnetic correlation function is given by $\tilde{G}(p) = (p^2+m^2)^{-1}$, one can easily find that $\xi_{\rm o}/\xi = \sqrt{1/6} = 0.408\,248\cdots$.

J. Stat. Mech. (2010) P03006

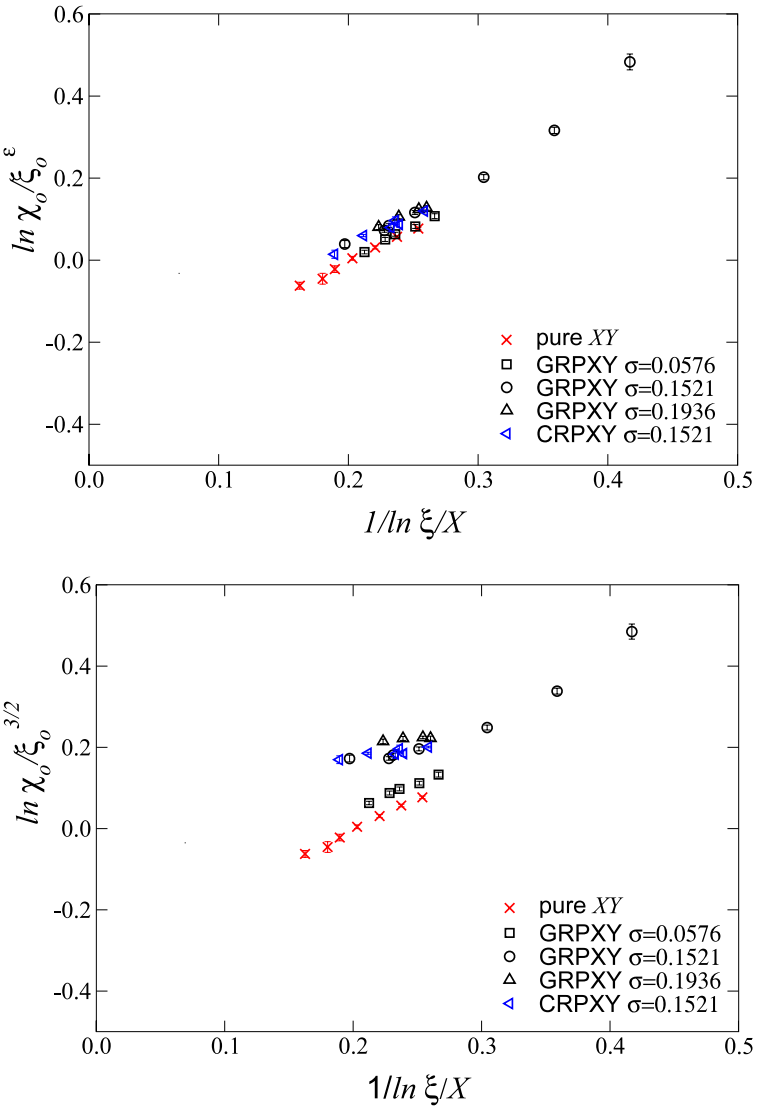

Figure 11. MC estimates of $\chi_{\rm o}/\xi_{\rm o}^{\varepsilon(\sigma)}$ (above), where $\varepsilon(\sigma) = 2 - \eta_{\rm o}(\sigma)$, and $\eta_{\rm o}(\sigma)$ is given by (33) and (34), and of $\chi_{\rm o}/\xi_{\rm o}^{2-\eta_{\rm o}}$ (below), where we take the pure XY exponent $\eta_{\rm o} = 1/2$.

Our MC estimates of the magnetic correlation length ξ are consistent with an exponential increase, i.e. with a behavior of the form $\ln \xi \sim t^{-1/2}$ with $t = T/T_{\rm M} - 1$; see figure 6. A linear fit to

$$\ln \xi = a t^{-1/2} + b \tag{35}$$

of the data satisfying $\xi \gtrsim 5$ gives the estimate

$$T_{\rm M} = \sigma_{\rm M} = 0.307(2), \tag{36}$$

with $\chi^2/{\rm DOF} \lesssim 1.0$. We also mention that fits to $\xi = a t^{-b}$ and to $\ln \xi = a t^{-1} + b$ give rise to a significantly larger χ^2.

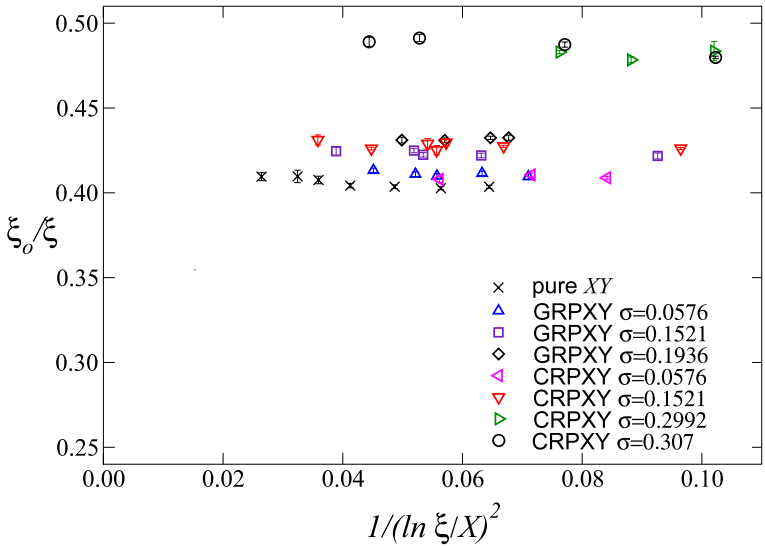

Figure 12. The ratio ξ_o/ξ versus $1/(\ln \xi/X)^2$ for the models considered.

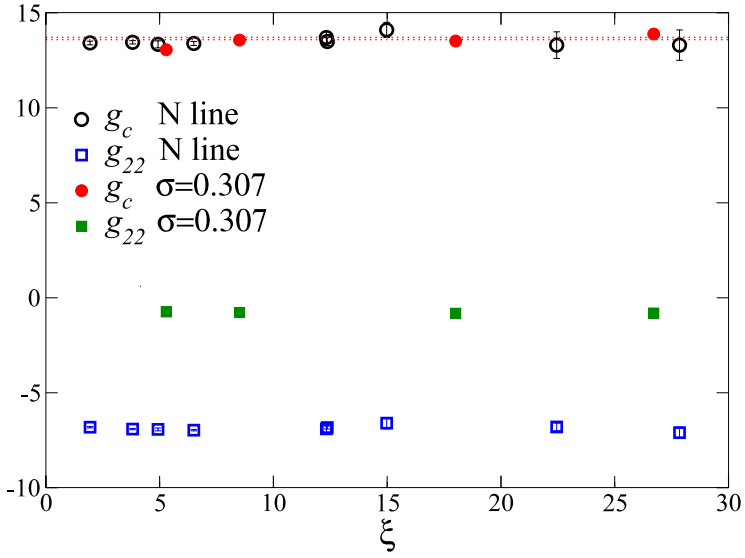

Figure 13. Estimates of g_c and g_{22} along the N line and at $\sigma = 0.307$. The dotted lines indicate the estimate [68] $g_c^* = g_{4,XY}^* = 13.65(6)$ for the pure XY model.

In order to estimate the exponent η, we fit χ and ξ to $\chi = c\xi^{2-\eta}$. Considering the MC results satisfying $\xi \gtrsim \xi_{\rm min} = 5$, we find $\eta = 0.246(4)$ with $\chi^2/{\rm DOF} \approx 1.0$. If we increase $\xi_{\rm min}$, η slightly decreases, but it is always compatible with $\eta = 1/4$. These results suggest that $\eta = 1/4$ also along the N line.

Figure 13 shows the estimates of g_c. The critical limit of g_c is consistent with the results for the pure XY model and those obtained along the thermal paramagnetic–QLRO line at smaller values of σ; see figure 8. Indeed, a fit of all data for g_c to (29) gives $g_c^* = 13.49(13)$ with $\chi^2/{\rm DOF} \approx 0.6$. If we consider only the data satisfying $\xi \gtrsim 4$, we obtain $g_c^* = 13.6(3)$.

J. Stat. Mech. (2010) P03006

The above-reported results (KT behavior of ξ, $\eta = 1/4$, and $g_c^* \approx g_{4,XY}^*$) suggest that the magnetic correlations behave as in the pure XY model. There is, however, a result which contradicts this hypothesis. As we discussed in section 4.1, the rate of approach of $\chi\xi^{-7/4}$ to its limiting value should be universal. As can be seen from figure 7, this is not the case: the slope of the data along the N line is clearly different from that predicted for the pure XY model. Thus, even though at the Nishimori point the magnetic critical behavior is the same as that observed along the thermal paramagnetic–QLRO transition line, the corrections are different, implying the presence of a new (probably marginal) RG operator, which only contributes to scaling corrections in magnetic quantities.

Better evidence for the presence of a new, disorder-related operator is obtained by considering g_{22} and ξ_o/ξ. In figure 13 we also report estimates of g_{22} along the N line and along the line $\sigma = 0.307$. If the estimate (36) is correct, the two lines intersect the critical line at the same point, the Nishimori point. It is quite clear from the data that the limiting values of g_{22} along the two lines are quite different. A fit of all available data on the Nishimori line to $g_{22}^* + b/(\ln \xi/X)^2$ gives $g_{22}^* = -7.00(5)$ with $\chi^2/\mathrm{DOF} \approx 0.9$. On the other hand, a fit of the data along the line at fixed $\sigma = 0.307$ gives $g_{22}^* \simeq -0.8$. The same phenomenon is observed for the ratio ξ_o/ξ. As can be seen in figure 12, for $\sigma = 0.307$ this ratio is approximately equal to 0.49, which is clearly different from the result that holds exactly along the Nishimori line, $\xi_o/\xi = 1$. The large differences of the values of these two RG invariant quantities along the two lines provide compelling evidence that the Nishimori point is a multicritical point as in the 2D $\pm J$ Ising model [60].

To understand this conclusion, let us review the basic results that apply to multicritical points. The singular part of the free energy should obey a scaling law

$$\mathcal{F}_{\mathrm{sing}}(u_1, u_2) = b^{-d}\mathcal{F}_{\mathrm{sing}}(b^{y_1}u_1, b^{y_2}u_2), \tag{37}$$

where u_1 and u_2 are two relevant scaling fields. They can be inferred by using the following facts: (i) the transition line at M must be parallel to the T axis, since it has been proved [8] that σ_{M} is an upper bound for the values of σ where QLRO can exist; (ii) the condition $T = \sigma$ at the N line is RG invariant. We therefore have

$$u_1 = \sigma - \sigma_{\mathrm{M}} + \cdots \tag{38}$$

where the dots indicate nonlinear corrections, which are quadratic in $\Delta\sigma \equiv \sigma - \sigma_{\mathrm{M}}$ and $\Delta T \equiv T - T_{\mathrm{M}}$, so the line $u_1 = 0$ runs parallel to the T axis at M. Moreover, we choose

$$u_2 = T - \sigma, \tag{39}$$

so the N line corresponds to $u_2 = 0$.

Close to the multicritical point, any RG invariant quantity, such as g_{22}, is expected to behave as

$$R = f_R(u_1 u_2^{-y_1/y_2}). \tag{40}$$

Now, the N line corresponds to $u_2 = 0$, so a RG invariant quantity converges to $f_R(\infty)$. On the other hand, the line $\sigma = \sigma_{\mathrm{M}}$ corresponds to $u_1 = 0$, so a RG invariant quantity converges to $f_R(0)$ which is generically expected to be different from $f_R(\infty)$. Thus, if the Nishimori point is multicritical, we expect RG invariant quantities to have different critical values along the two lines. This is exactly what we observe for g_{22} and ξ_o/ξ. Thus,

J. Stat. Mech. (2010) P03006

in view of the numerical results we conclude that the Nishimori point is a multicritical point.

It is interesting to note that the multicritical behavior is not observed in the magnetic sector. For instance, $g_{\rm c}^*$ along the paramagnetic–QLRO line is equal to its XY value $g_{4,XY}^*$. The same result holds along the Nishimori line. In terms of the scaling function $f_{g_{\rm c}}$ defined in (40) these results imply

$$f_{g_{\rm c}}(0) = f_{g_{\rm c}}(\infty) = g_{4,XY}^*. \tag{41}$$

It is then natural to conjecture that $g_{\rm c}^* = g_{4,XY}^*$ along any line that intersects the Nishimori point, i.e. that $f_{g_{\rm c}}(x) = g_{4,XY}^*$ for any x. The absence of multicritical behavior in the magnetic sector is also supported by the fact that ξ always shows a KT behavior and that the magnetic exponent η at the Nishimori point is equal to the pure XY value 1/4.

The results that we have presented should apply to the generic RP XY model. In all cases we expect a multicritical point along the paramagnetic–QLRO transition line. It follows from universality that, at the multicritical point, the magnetic and the overlap correlation functions have the same critical behavior—hence, we have $\eta = \eta_{\rm o}$—though they may not be necessarily equal as is the case for the CRP XY model. Note that this point is not expected in general to coincide with that at which the tangent to the transition line is parallel to the T axis.

6. Glassy critical behavior at $T = 0$

In the limit $\sigma \to \infty$ the RP XY model corresponds to the gauge-glass model in which the phase shifts are uniformly distributed. This model has been extensively studied both at zero and at finite temperature [5, 10], [14]–[19], [21, 22, 25, 26, 29], [32]–[34], [36, 38, 40, 41], [43]–[54]. References [21, 22] showed that no long-range glassy order can exist at finite temperature. Although this result does not exclude the possibility of a finite-temperature transition with an exotic low-temperature glassy phase, for example a phase characterized by glassy QLRO, most numerical works [5, 19, 36, 43, 45, 46], [49]–[51] support a zero-temperature glassy critical behavior. The overlap correlation length $\xi_{\rm o}$ diverges as $T^{-\nu}$ for $T \to 0$. We mention the estimates [45] $1/\nu = 0.39(3)$ and [49] $1/\nu = 0.36(3)$ from finite-temperature MC simulations, and [43] $1/\nu = 0.36(1)$ and [51] $1/\nu \approx 0.45$ from $T = 0$ numerical calculations. Moreover, if one assumes that the ground state is nondegenerate in the overlap variables, one obtains that at $T = 0$ the finite-size overlap susceptibility satisfies the relation $\chi_{\rm o} = L^2$, so $\eta_{\rm o} = 0$. We mention that this scenario was questioned in [40, 41, 44, 47, 48], [52]–[54], which claimed the existence of a finite-temperature transition at $T \approx 0.2$.

A natural scenario for the phase digram of the GRP XY and CRP XY models is that the glassy transition, which occurs for $\sigma = \infty$, is not isolated but that it is the endpoint of a phase transition line that starts at the paramagnetic–QLRO transition line. In particular, if the zero-temperature glassy transition scenario applies to the gauge-glass model, we expect a line of $T = 0$ glassy transitions for any $\sigma > \sigma_{\rm D}$; see figure 1. A natural conjecture would be that all these transitions belong to the same universality class.

To check this scenario we performed MC simulations of the CRP XY model at $\sigma = 2/3, 5/9, 1/2, \infty$, which are larger than $\sigma_{\rm D} \leq \sigma_{\rm M} \approx 0.31$. As we shall see, the results clearly support a glassy $T = 0$ transition in the same universality glass as that of the gauge-glass model.

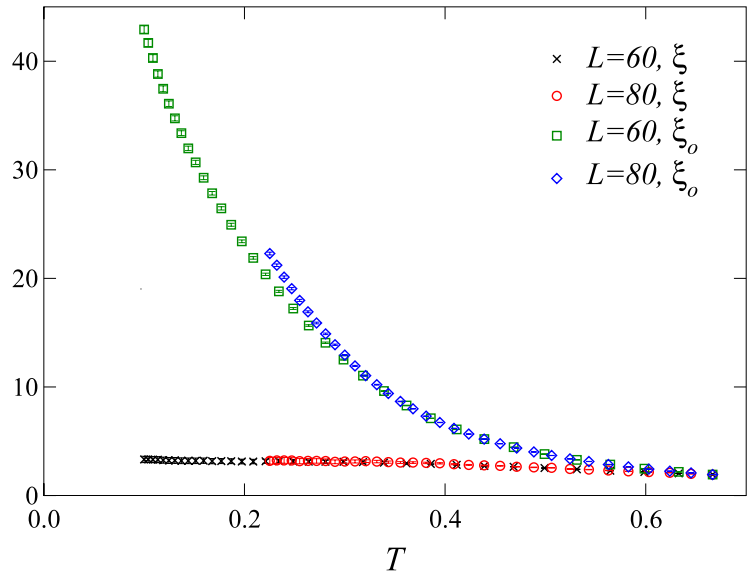

Figure 14. MC estimates of the correlation lengths ξ and ξ_o for the CRP XY model at $\sigma = 2/3$.

6.1. MC simulations

We performed MC simulations of the CRP XY model on square $L\times L$ lattices with periodic boundary conditions. Most of the results that we shall present refer to runs with $\sigma = 2/3$. In this case we considered $L = 20$, 30, 40, 60, 80 and temperatures between $T = 2/3$ (at the Nishimori line) and $T = 0.1$ (for $L = 80$ we considered $0.22 \leq T \leq 2/3$). We averaged over a relatively large number N_s of samples: $N_s = 6000$, 9000, 7000, 3000, and 2000 samples for $L = 20$, 30, 40, 60 and 80, respectively. We used the MC algorithm discussed in appendix A combined with the parallel-tempering method [71, 72]. Moreover, to check the universality of the transitions, we also performed parallel-tempering MC simulations for $\sigma = 5/9$ and lattice sizes $L = 60, 70$ (5000 and 1000 disorder samples, respectively), $\sigma = 1/2$ and $L = 70$ (1000 samples), and $\sigma = \infty$ and $L = 20$, 30, 40, 60 (5000, 5000, 2000, 2000 samples, respectively). The points in the T–σ plane where we collected MC data are shown in figure 3.

At the glassy transition the critical modes are those related to the overlap variables, while the magnetic ones are noncritical. This is clearly shown in figure 14, which shows ξ and ξ_o for $\sigma = 2/3$. The overlap correlation length ξ_o increases steadily with decreasing temperature, while the magnetic correlation length ξ freezes at sufficiently low temperatures at a value $\xi \approx 3.3$. Therefore, the critical temperature and exponents must be determined from quantities related to the overlap correlation functions.

6.2. Evidence for a $T = 0$ glassy transition at $\sigma = 2/3$

In order to determine the critical temperature, we analyze $R_{\xi_o} \equiv \xi_o/L$. The results, shown in figure 15, show no evidence of a crossing point in the range of values of T of the data, $T \geq 0.1$, and thus provide the bound $T_c < 0.1$ for the critical temperature T_c. A more precise determination of T_c can be obtained by a finite-size scaling (FSS) analysis. We fit

J. Stat. Mech. (2010) P03006

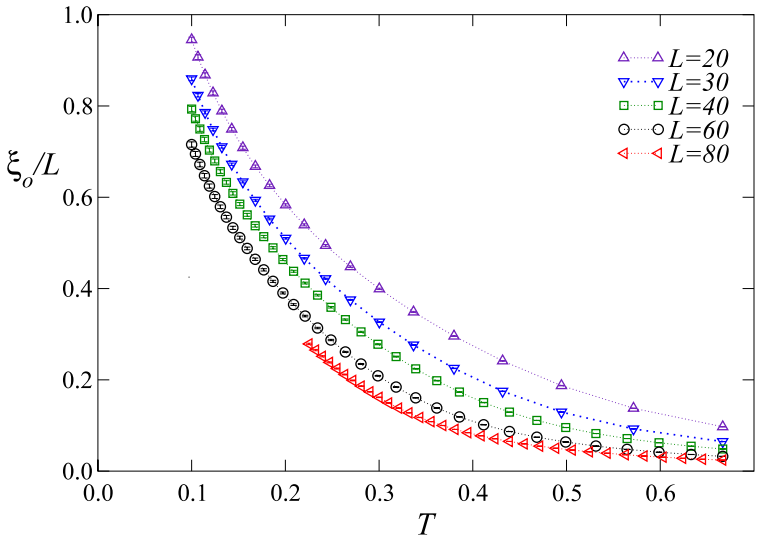

Figure 15. MC estimates of the ratio $R_{\xi_o} \equiv \xi_o/L$ for the CRP XY model at $\sigma = 2/3$.

the data to

$$R_{\xi_o} = P_n[(T - T_c)L^{1/\nu}], \tag{42}$$

keeping T_c and ν as free parameters. Here $P_n(x)$ is a polynomial in x of order n. The order n is fixed by looking at the χ^2 of the fit. For each n we determine the goodness of the fit, $\chi^2(n)$. Then, we fix n such that $\chi^2(n)$ is not significantly different from $\chi^2(n+1)$. The results that we report correspond to $n = 6$. To identify the role of the corrections to scaling we repeat the fit several times. Each time we fix two parameters $T_{\max}$ and $L_{\min}$ and we only include the data which correspond to lattices satisfying the conditions $T \le T_{\max}$ and $L \ge L_{\min}$.

In table 1 we report the estimates of T_c for several values of $T_{\max}$ and $L_{\min}$. We obtain estimates of T_c which are quite small and satisfy the upper bound

$$T_c \lesssim 0.01. \tag{43}$$

Since our data satisfy $T \ge 0.1$, this estimate allows us to conclude that our results are fully consistent with a zero-temperature transition. From now on, we always assume $T_c = 0$.

6.3. The critical exponent ν

In order to determine the critical exponent ν related to the divergence of the correlation length ξ_o, we repeat the fit (42) at $\sigma = 2/3$ setting $T_c = 0$. The results are reported in table 2. They slightly increase as $T_{\max}$ or $L_{\min}$ is lowered, but these changes are small compared to the statistical errors.

In fit (42) we made two approximations. First, we neglected the nonanalytic scaling corrections, which decrease as $L^{-\omega}$. The results indicate that these corrections are small: at fixed $T_{\max} < 0.25$ the estimates of ν obtained setting $L_{\min} = 30$ and 40 differ by much less than the statistical errors. Second, we approximated the thermal nonlinear scaling

J. Stat. Mech. (2010) P03006

Table 1. Estimates of T_c obtained by fitting R_ξ to (42) with $n = 6$. DOF is the number of degrees of freedom of the fit.

L_{min}	T_{max}	χ^2/DOF	T_c
20	0.6	169/157	0.018(1)
20	0.5	99/141	0.009(1)
20	0.4	67/119	0.010(2)
20	0.3	30/92	0.010(3)
30	0.6	137/138	0.017(1)
30	0.5	66/123	0.008(2)
30	0.4	49/103	0.007(3)
30	0.3	21/79	0.005(4)
40	0.6	106/119	0.017(2)
40	0.5	42/105	0.007(2)
40	0.4	31/87	0.007(3)
40	0.3	17/66	0.007(5)

Table 2. Estimates of ν obtained by fitting R_{ξ_o} to (42) with $T_c = 0$ and $n = 6$. DOF is the number of degrees of freedom of the fit.

L_{min}	T_{max}	χ^2/DOF	ν
20	0.4	100/120	2.465(6)
20	0.3	44/93	2.496(10)
20	0.25	24/77	2.528(14)
20	0.2	17/55	2.547(22)
20	0.16	14/39	2.548(31)
30	0.4	55/104	2.446(6)
30	0.3	23/80	2.464(13)
30	0.25	13/65	2.489(20)
30	0.2	10/46	2.492(30)
30	0.16	9/32	2.488(42)
40	0.4	36/88	2.432(7)
40	0.3	19/67	2.451(15)
40	0.25	12/53	2.480(26)
40	0.2	8/37	2.490(38)
40	0.16	9/25	2.482(53)

field u_T by $u_T \approx T$, neglecting the *analytic* corrections (see [73] for an extensive discussion of such corrections). To understand their quantitative role, we performed fits to

$$R_\xi = P_n(u_T L^{1/\nu}), \qquad u_T \equiv T + pT^2, \tag{44}$$

where p is a new free parameter. The results are reported in table 3. Corrections are tiny and we estimate $|p| \lesssim 0.2$, so $|u_T - T|/T$ is at most 0.10, 0.02 for $T = 0.5$, 0.1, respectively. The estimates of ν do not vary significantly and, for $L \geq 30$ and $T_{max} \leq 0.2$, are fully consistent with those obtained before. We quote

$$\nu = 2.5(1), \qquad 1/\nu = 0.40(2) \tag{45}$$

as our final estimate.

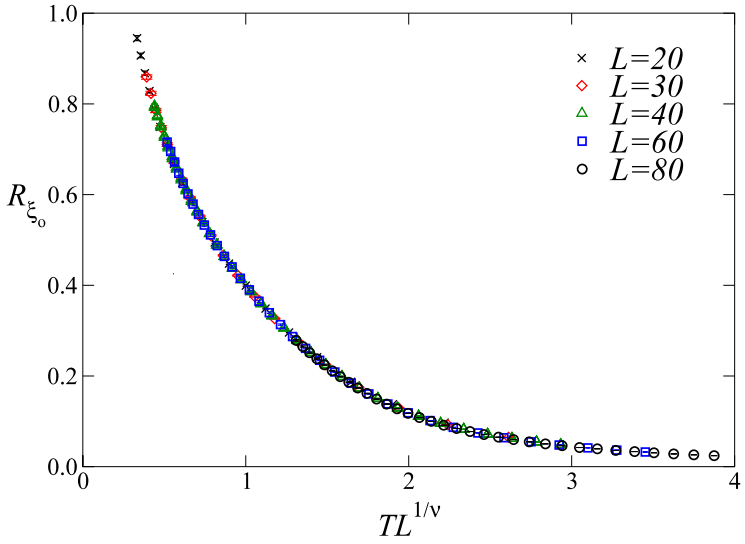

Figure 16. $R_{\xi_o} \equiv \xi_o/L$ versus $TL^{1/\nu}$ for $\nu = 2.5$; data corresponding to $\sigma = 2/3$.

Table 3. Estimates of ν and p obtained by fitting R_{ξ_o} to (44) with $n = 6$. DOF is the number of degrees of freedom of the fit.

$L_{\min}$	$T_{\max}$	χ^2/DOF	ν	p
20	0.5	98/141	2.54(1)	−0.11(1)
20	0.4	63/119	2.62(2)	−0.20(2)
20	0.3	28/92	2.71(4)	−0.34(5)
20	0.25	20/76	2.67(6)	−0.26(11)
20	0.2	16/54	2.67(10)	−0.29(21)
30	0.5	89/123	2.42(2)	−0.00(2)
30	0.4	47/103	2.54(2)	−0.12(3)
30	0.3	20/79	2.58(5)	−0.18(7)
30	0.25	13/64	2.54(7)	−0.11(14)
30	0.2	10/45	2.50(12)	−0.01(31)
40	0.5	50/105	2.42(2)	−0.00(2)
40	0.4	31/87	2.50(3)	−0.09(3)
40	0.3	17/66	2.58(6)	−0.20(7)
40	0.25	12/52	2.54(16)	−0.12(16)
40	0.2	10/36	2.50(13)	−0.01(33)

To show the quality of our FSS results in figure 16 we plot R_ξ versus $TL^{1/\nu}$, using the estimate (45). All data fall on top of each other with remarkable precision.

6.4. The critical exponent η_o

As discussed at length in [73], the overlap susceptibility behaves in the critical limit as

$$\chi_o = \bar{u}_h^2 L^{2-\eta_o} f(u_T L^{1/\nu}). \tag{46}$$

Here u_T is the temperature nonlinear scaling field, while $\bar{u}_h$ is related to the external *overlap–magnetic* scaling field u_h associated with the overlap variables by $u_h = h\bar{u}_h(T) +$

Table 4. Estimates of η_o. On the left we report the results of the fits to (48) with $n = 6$, on the right those to (49) with $n = 6$ and $m = 2$. In both cases we fix $\nu = 2.5(1)$. The reported errors are the sums of the statistical errors and of the variations of the estimate of η_o as ν changes by one error bar. DOF is the number of degrees of freedom of the fit.

		Fit (48)		Fit (49)	
$L_{\min}$	$T_{\max}$	χ^2/DOF	η_o	χ^2/DOF	η_o
20	0.5	11 570/142	0.13(2)	338/140	−0.01(1)
20	0.4	1439/120	0.10(2)	99/118	0.02(1)
20	0.3	498/93	0.06(1)	39/91	0.04(3)
20	0.25	182/77	0.06(1)	20/75	0.01(3)
20	0.2	43/55	0.05(1)	12/53	−0.04(8)
30	0.5	6592/124	0.17(2)	263/122	−0.03(2)
30	0.4	1096/104	0.11(2)	78/102	0.01(2)
30	0.3	330/80	0.07(1)	35/78	0.04(3)
30	0.25	89/65	0.05(1)	18/63	0.00(4)
30	0.2	28/46	0.05(2)	11/44	−0.06(10)
40	0.5	4237/106	0.18(2)	177/104	−0.05(2)
40	0.4	1096/88	0.11(2)	40/86	−0.03(2)
40	0.3	294/67	0.07(1)	22/65	0.02(4)
40	0.25	63/53	0.05(1)	9/51	−0.02(6)
40	0.2	17/37	0.04(1)	2/35	−0.11(12)

$O(h^2)$. We have already checked that the thermal scaling field u_T can be effectively approximated by $u_T = T$. Thus, neglecting nonanalytic scaling corrections, the data should behave as

$$\ln \chi_o = (2 - \eta_o) \ln L + \ln \bar{u}_h(T)^2 + \ln f(TL^{1/\nu}). \tag{47}$$

We now estimate η_o from the analysis of the data at $\sigma = 2/3$. In a first set of fits we set $\bar{u}_h = 1$ and approximate $\ln f(x)$ with a polynomial in x of order n, i.e., we perform fits to

$$\ln \chi_o = (2 - \eta_o) \ln L + P_n(TL^{1/\nu}). \tag{48}$$

The analysis of the χ^2 of the fits indicate that $n = 6$ allows us to describe the data accurately. We fix ν to the estimate (45) to avoid having an additional nonlinear parameter in the fit. The results are reported in table 4. We observe a significant change of the estimates as $T_{\max}$ decreases; moreover, the quality of the fit is quite poor. This can be explained by the presence of sizable analytic corrections, which means that $\bar{u}_h$ is poorly approximated by $\bar{u}_h = 1$ in our range of temperatures. The same phenomenon occurs for the three-dimensional Ising spin glass [73], where the analytic corrections cannot be neglected in the analysis of the overlap susceptibility. We thus perform a second set of fits in which we take into account the magnetic nonlinear scaling field. If we approximate $\ln \bar{u}_h^2$ with a polynomial of order m, we end up with the fitting form

$$\ln \chi_o = (2 - \eta_o) \ln L + P_n(TL^{1/\nu}) + Q_m(T), \tag{49}$$

J. Stat. Mech. (2010) P03006

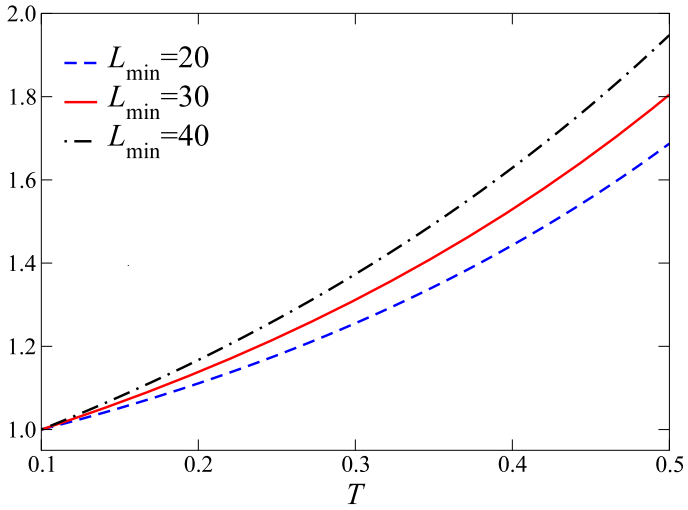

Figure 17. Plot of the ratio $\bar{u}_h(T)/\bar{u}_h(T=0.1)$ from fits with $T_{\rm max}=0.5$ and $L_{\rm min}=20$, 30, 40.

where we assume $Q_m(0)=0$. In the following we take $m=2$ and again fix ν to the estimate (45). The results are reported in table 4. The quality of the fit is now significantly better, indicating that the analytic corrections are important. The scaling function $\bar{u}_h$ is reported in figure 17 and it does indeed vary significantly in the range of values of T that we are considering. The estimates of $\eta_{\rm o}$ do not show any systematic variation with $T_{\rm max}$ and are always consistent, within errors, with $\eta_{\rm o}=0$. Quantitatively, our data allow us to set the upper bound

$$|\eta_{\rm o}| \leq 0.05. \tag{50}$$

6.5. Results for the gauge-glass model

In order to check universality we also performed runs at $\sigma=\infty$, although in this case we considered smaller lattices and the errors are significantly larger (partly because of the smaller number of samples, partly because of larger sample-to-sample fluctuations). The data were analyzed as we did in the $\sigma=2/3$ case. First, we determined the critical temperature $T_{\rm c}$. A fit of $\xi_{\rm o}/L$ to (42) gives rather small estimates of $T_{\rm c}$. For $L_{\rm min}=20$ we obtain $T_{\rm c}=0.030(2)$ (resp., 0.020(3)) for $T_{\rm max}=0.4$ (resp., 0.3). Thus, we can conclude that $T_{\rm c} \lesssim 0.02$, which is clearly consistent with $T_{\rm c}=0$, given that our data belong to the range $T \geq 0.1$. The claim that $T_{\rm c} \approx 0.2$ is not consistent with our MC data.

Then, we determined ν by assuming $T_{\rm c}=0$. The results of the fits to (42) show a significant dependence on $T_{\rm max}$. For $L_{\rm min}=20$, ν varies between 2.50(1) and 2.80(4) as $T_{\rm max}$ varies between 0.4 and 0.16. If analytic scaling corrections are included, i.e. we fit the data to (44), we observe a significantly smaller dependence on $T_{\rm max}$, but, on the other hand, a rather large dependence on $L_{\rm min}$, with rapidly increasing error bars as $L_{\rm min}$ increases. This is probably due to the fact that we have a somewhat large statistical error on the results with the largest value of L, $L=60$. The estimates of ν vary between 2.8 and

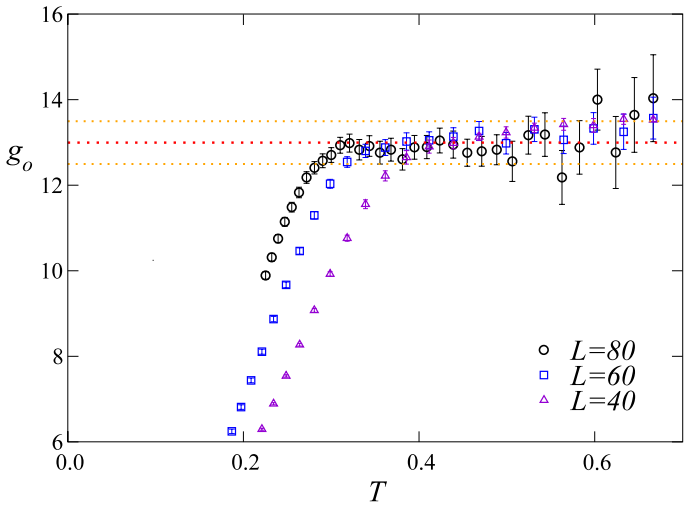

Figure 18. MC estimates of g_o versus T at $\sigma = 2/3$ for $L = 40, 60, 80$. The dotted lines correspond to the infinite-volume critical ($T = 0$) estimate $g_o^* = 13.0(5)$.

3.7 if we take $L_{\rm min} = 20$, 30 and $0.2 \le T_{\rm max} \le 0.5$ and thus give the final result $\nu = 3.3(5)$. This result is somewhat larger than the estimate (45), but certainly not inconsistent. It supports—very weakly, though—universality. A better check is presented below.

6.6. The quartic coupling g_o and universality

We computed the overlap quartic coupling g_o defined in (16). MC results at $\sigma = 2/3$ are shown in figure 18. The infinite-volume limit, within our statistical accuracy, is apparently reached when $L/\xi_o \gtrsim 7$, corresponding to $T \gtrsim 0.3$ for our largest lattices $L = 60, 80$. The infinite-volume results are quite stable with respect to T, so we can reliably estimate the critical ($T = 0$) value g_o^*. We obtain

$$g_o^* = 13.0(5). \tag{51}$$

According to standard RG arguments, g_o has a universal FSS limit as a function of $R_{\xi_o} \equiv \xi_o/L$, that is

$$g_o(T, L) = f(R_{\xi_o}), \tag{52}$$

where the function $f(x)$ is universal and satisfies $f(0) = g_o^*$. This scaling behavior is nicely supported by the data at $\sigma = 2/3$ for various lattice sizes; see figure 19. Universality can be checked by also considering the results for $\sigma = 5/9$, $\sigma = 1/2$ and $\sigma = \infty$. Clearly, all points fall on top of each other. Note that here there are no free parameters to fiddle with and thus this comparison provides strong support to the hypothesis that all these models belong to the same universality class. Given the very good evidence that we have that the model with $\sigma = 2/3$ undergoes a $T = 0$ glassy transition, this result further confirms (and provides evidence stronger than that given in the previous paragraph showing) that the gauge-glass model does not have a finite-temperature exotic glassy transition.

J. Stat. Mech. (2010) P03006

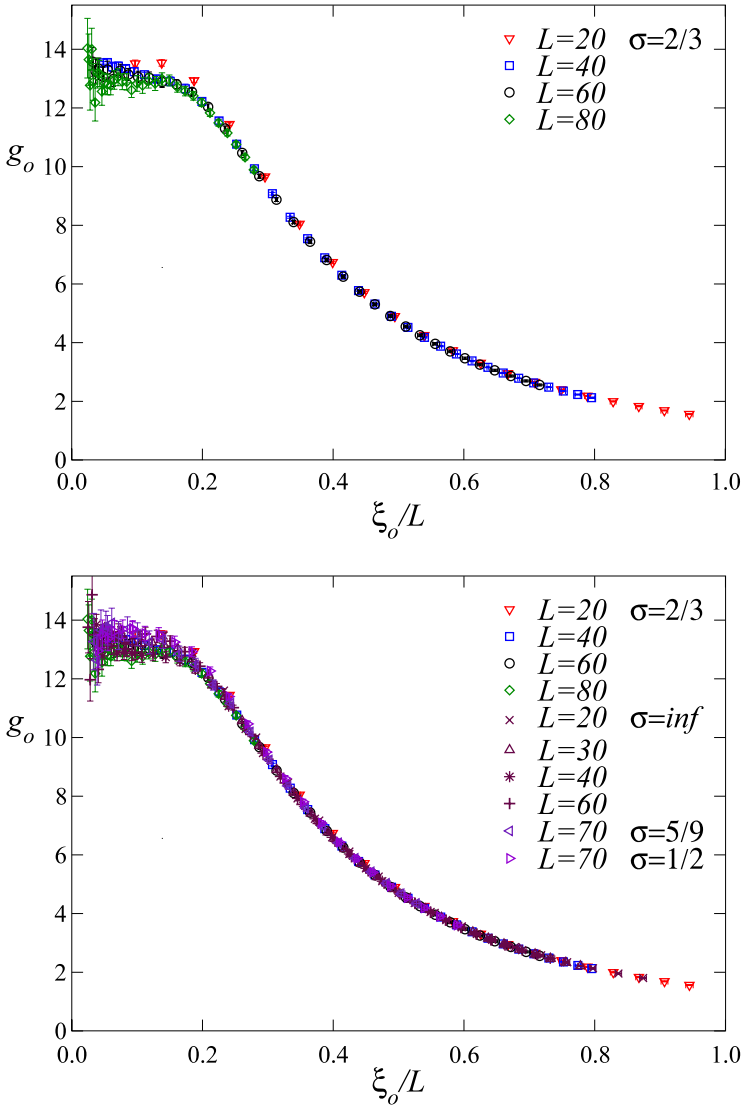

Figure 19. g_o versus $R_{\xi_o} \equiv \xi_o/L$: data at $\sigma = 2/3$ for various lattice sizes $L = 20, 40, 60, 80$ (above), and including (below) also data for other values of σ: $\sigma = 5/9, 1/2, \infty$.

6.7. Behavior of the magnetic correlation functions

Let us now consider the magnetic quantities. The magnetic correlation length ξ is zero in the gauge-glass model (see appendix E), and increases as one approaches the QLRO region. In particular, at $T = 0.159$, which is below the critical temperature $T_M \approx 0.31$ along the Nishimori line, we obtain $\xi = 3.3(1), 6.7(4), 9.8(3)$ at $\sigma = 2/3, 5/9, 1/2$, respectively. These values are roughly consistent with a behavior like $\ln \xi \sim (\sigma - \sigma_c)^{-\kappa}$ assuming $\sigma_c \approx \sigma_M \approx 0.30$, i.e., with a KT-like behavior along the transition line that connects the Nishimori critical point M (see figure 1), and the $T = 0$ transition point at $\sigma = \sigma_D$, which is expected to run almost parallel to the T axis. Note, however, that while our data suggest a power-law divergence of $\ln \xi$ (and therefore, ξ has an exponential divergence),

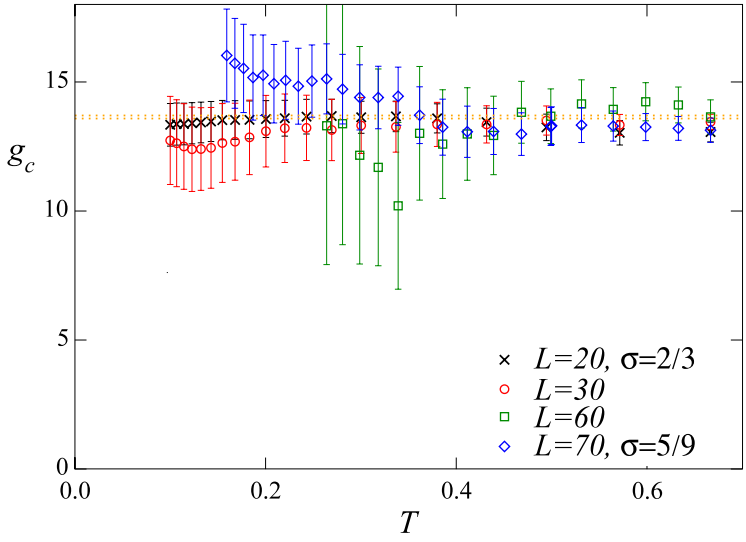

Figure 20. MC estimates of the quartic couplings g_c. The dotted line corresponds to the XY value $g_c = g_4 = 13.65(6)$.

they are not sufficiently precise to allow us to estimate the power κ. The KT value $\kappa = 1/2$ is consistent with the data, but $\kappa = 1$ would be equally reasonable.

It is also interesting to discuss the behavior of the quartic couplings g_c, g_4, and g_{22} defined from the magnetic correlation functions in (13)–(15). In appendix E, assuming universality, we predict that, in the critical limit, g_4 and g_{22} should diverge as ξ_o^2, while $g_c \xi_o^{-2}$ should go to zero.

Numerical estimates of g_c are shown in figure 20. The results are clearly consistent with a finite $T = 0$ limit. Note that the estimates obtained for $\sigma = 2/3$, $5/9$, and $1/2$ are close to the XY value $g^*_{4,XY} = 13.65(6)$; actually, they are consistent within errors, even at small T, below $T_M \approx 0.31$. These results are suggestive of a KT behavior of the magnetic correlation functions also along the disorder paramagnetic–QLRO transition line from M to D; see figure 1. Indeed, for $\sigma = 2/3$, $5/9$, $1/2$ we have $\xi \approx 3$, 7, 10, so along these lines one should be able to observe the critical behavior that arises when one approaches the paramagnetic–QLRO transition line at a point with $T < T_M$. In other words, these results imply that the critical limit of $g_c(\sigma, T)$ at fixed $T < T_M$ along the paramagnetic–QLRO transition line is consistent with the KT value. This fact provides some evidence that also along the disorder-driven transition line magnetic correlation functions behave as in the pure XY model. Of course, as σ increases (and thus, the magnetic correlation length ξ decreases), g_c changes significantly and, for $\sigma = \infty$, g_c is infinite for any T and L.

The couplings g_{22} and g_4 are instead expected to diverge as ξ_o^2. In figure 21 we report g_{22} for the different models. The data are clearly diverging as $\xi \to \infty$, but the asymptotic behavior $g_{22} \sim \xi_o^2$ is not clearly observed, likely because the values of ξ_o are not sufficiently large. Indeed, we only observe that g_{22} behaves as ξ_o^κ with κ rapidly increasing with ξ_o. More precisely, if we only include data satisfying $\xi_o \lesssim 10$ we obtain $\kappa \approx 1$. If instead we fit the data with $10 \lesssim \xi_o \lesssim 20$ (we have infinite-volume data only up to $\xi_o \approx 20$) we obtain $\kappa \approx 1.5$.

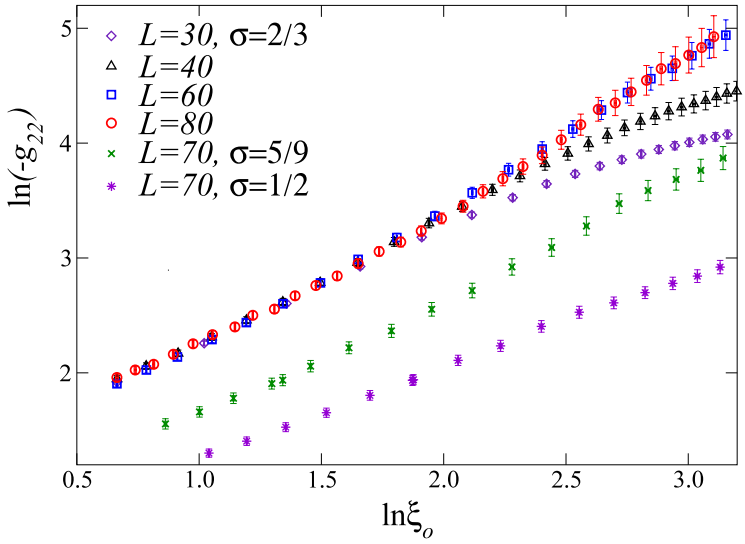

Figure 21. Plot of $\ln(-g_{22})$ versus $\ln \xi_{\rm o}$ at $\sigma = 2/3, 5/9, 1/2$.

7. Conclusions

We have studied the magnetic and glassy transitions of the square-lattice XY model in the presence of random phase shifts and, in particular, the GRP XY and CRP XY model defined by the distributions (2) and (3). The latter is very useful because it allows some exact calculations along the Nishimori line $T = \sigma$ [8, 9], where, in particular, the magnetic and overlap two-point functions are equal. We present MC results for the GRP XY and CRP XY models for several values of the temperature and of the parameter σ controlling the disorder, approaching the magnetic and glassy transition lines from the paramagnetic phase. We substantially confirm the phase diagram shown in figure 1.

Our main results are the following.

(i) We have carefully investigated the critical behavior along the transition line separating the paramagnetic and QLRO phases, from the pure XY point P to the multicritical point, which, in the CRP XY model, lies on the N line and is such that the transition line runs parallel to the T axis. The magnetic observables show a σ independent KT behavior: the magnetic correlation length behaves as $\ln \xi \sim u_{\rm t}^{-1/2}$, where $u_{\rm t}$ is the thermal scaling field, $u_{\rm t} \sim T - T_{\rm c}(\sigma)$, and the magnetic susceptibility as $\chi \sim \xi^{7/4}$ (corresponding to $\eta = 1/4$). Moreover, the quartic coupling $g_{\rm c}$ defined in (15) appears to be universal. We obtain $g_{\rm c}^* \approx 13.6$, which is nicely consistent with the corresponding value $g_{4,XY}^* = 13.65(6)$ of the pure XY model [68, 70]. We have also verified the universality of the leading logarithmic correction to the critical behavior of χ. On the other hand, the critical behavior of disorder-related quantities, such as those related to the overlap correlation function, depends on σ.

(ii) In the CRP XY model, the Nishimori point M (see figure 1) is a multicritical point which divides the paramagnetic–QLRO line into two parts: a thermally driven transition line (from P to M) and a disorder-driven transition line (from M to D). This result should be general: a multicritical point should also exist in generic RP

XY models, although in this case it is not expected to coincide with that where the transition line runs parallel to the T axis. Such a multicritical point is characterized by the fact that, at criticality, magnetic and overlap functions have the same critical behavior, that is $\eta = \eta_o$: in the CRP XY model the two correlation functions are exactly equal (more generally, they are equal on the whole N line), but we do not expect this property to be generic. It is interesting to observe that the multicritical behavior is only observed in the disorder-related quantities. Magnetic observables behave, as far as the leading behavior is concerned, as in the pure XY model: the correlation length shows a KT behavior, $\eta = 1/4$, and $g_c^* = g_{4,XY}^*$ in the whole neighborhood of the multicritical point. However, corrections are different from those appearing in the pure XY model, providing additional evidence for the presence of an additional (probably marginal) RG operator, which is responsible for the multicritical behavior.

(iii) Little is known about the behavior along the transition line from the multicritical point to D. However, the fact that purely magnetic observables behave as in the pure XY model both along the thermally driven transition line and at the multicritical point leads us to conjecture that the magnetic behavior is also unchanged. We have presented some very weak evidence in section 6.7. We should mention that RG arguments [23] predict $\eta = 1/16$—clearly different from the KT value $\eta = 1/4$—at $\sigma = \sigma_D$ and $T = 0$. This result is not in contradiction with our conjecture. Indeed, the $T = 0$ point is the intersection of two different transition lines and therefore it is expected to be a multicritical point. Hence, the behavior for $T = 0$ may be different from that observed along the finite-temperature transition line.

(iv) We have investigated the critical behavior for large values of σ. We find no evidence of a finite-temperature transition for all values of σ that we have investigated: the system is paramagnetic up to $T = 0$, where a glassy transition occurs. Moreover, in all cases we confirm universality. We can thus conjecture that the critical behavior along the whole line that starts at D (see figure 1) is universal: for any $\sigma > \sigma_D$, one has the same critical behavior characterized by the exponents

$$\nu = 2.5(1), \qquad 1/\nu = 0.40(2), \qquad |\eta_o| \leq 0.05. \tag{53}$$

Our estimate of ν is consistent with earlier estimates obtained by MC simulations of the gauge-glass XY model, for example $1/\nu = 0.39(3)$ and $1/\nu = 0.36(3)$ obtained in [45] and [49] respectively, and by numerical calculations of the stiffness exponent at $T = 0$, for example $1/\nu = 0.36(1)$ and $1/\nu \approx 0.45$ obtained in [45] and [51]. Our result for η_o is consistent with a general argument which predicts $\eta_o = 0$.

Appendix A. Details for the Monte Carlo simulation

In the simulation we use both Metropolis and microcanonical local updates. The latter do not change the energy of the configuration and are defined as follows. Consider a site i; the corresponding field is ψ_i. The terms of the Hamiltonian that depend on ψ_i can be written as

$$\mathcal{H}_i = \mathrm{Re}(\bar{\psi}_i z), \qquad z \equiv \sum_j U_{ij}\psi_j, \tag{A.1}$$

where the sum is over all nearest neighbors j of site i. Then, define

$$\psi_i' = 2\frac{z}{|z|^2}\,\mathrm{Re}(\bar{\psi}_i z) - \psi_i. \tag{A.2}$$

One can verify that $|\psi_i'| = 1$ and that

$$\mathrm{Re}(\bar{\psi}_i z) = \mathrm{Re}(\bar{\psi}_i' z). \tag{A.3}$$

Thus, the update $\psi_i \to \psi_i'$ does not change the energy and can therefore always be accepted. This update does not suffer the limitations of the Metropolis update: ψ_i and ψ_i' are not close to each other.

In our simulation a MC step consists of five microcanonical sweeps over all of the lattice followed by one Metropolis sweep. For each disorder sample we typically perform $\mathrm{O}(10^5)$ MC steps. In some simulations of the CRP XY model we also use the parallel-tempering method [71, 72]. It allows us to obtain results for small values of T, in particular below the Nishimori line $T = \sigma$. In the parallel-tempering simulations we consider N_T systems at the same value of σ and at N_T different inverse temperatures $\beta_{\min} \equiv \beta_1, \ldots, \beta_{\max}$, where $\beta_{\max}$ corresponds to the minimum value of the temperature that we are interested in. The value $\beta_{\min}$ is chosen such that the thermalization at $\beta = \beta_{\min}$ is sufficiently fast, while the intermediate values β_i are chosen such that the acceptance probability of the temperature exchange is at least 5%. Moreover, we require that, for some i, $\beta_i = \sigma$. This allows us to collect data on the Nishimori line. The exact results valid on it allow us to check the correctness of the MC code and perform a (weak) test of thermalization. Thermalization is checked by verifying that the averages of the observables are independent of the number of MC steps for each disorder realization.

The overlap correlations and the corresponding χ_{o} and ξ_{o} are measured by performing two independent runs for each disorder sample. Finally, note that the determination of g_{22} defined in (14) requires the computation of the disorder average of products of thermal expectations. This should be done with care in order to avoid any bias due to the finite length of the run for each disorder realization. We use the essentially unbiased estimators discussed in [73, 74].

Appendix B. The KT RG equations

In this appendix we consider the RG flow for the sine–Gordon (SG) model, with the purpose of understanding its universal features. As a results we shall obtain the critical behavior of the correlation length and of the magnetic susceptibility at the KT transition. This appendix generalizes the results presented in [75]–[77]. The SG model is parameterized by two couplings, α and δ—we use the notation of [75, 77]—whose β functions are

$$\beta_\alpha = 2\alpha\delta + \tfrac{5}{64}\alpha^3 + \cdots, \tag{B.1}$$

$$\beta_\delta = \tfrac{1}{32}\alpha^2 - \tfrac{1}{16}\alpha^2\delta + \cdots, \tag{B.2}$$

where the dots indicate higher-order terms. To all orders the β functions have the generic form

$$\beta_\alpha = 2\alpha\delta + \sum_{n+m>2} b_{\alpha,nm}\alpha^n\delta^m, \tag{B.3}$$

$$\beta_\delta = \tfrac{1}{32}\alpha^2 + \sum_{n+m>2} b_{\delta,nm}\alpha^n\delta^m. \tag{B.4}$$

In the SG model the sign of α is irrelevant, which implies the symmetry relations

$$\beta_\alpha(\alpha,\delta) = -\beta_\alpha(-\alpha,\delta), \qquad \beta_\delta(\alpha,\delta) = \beta_\delta(-\alpha,\delta). \tag{B.5}$$

As a consequence, $b_{\alpha,nm} = 0$ if n is even and $b_{\delta,nm} = 0$ if n is odd. Moreover, for $\alpha = 0$ the theory is free and δ does not flow. Hence

$$\beta_\delta(\alpha = 0,\delta) = 0, \tag{B.6}$$

which implies $b_{\delta,nm} = 0$ if $n = 0$.

Let us now consider a general nonlinear analytic redefinition of the couplings

$$\alpha = a_{\alpha,10}u + \sum_{n+m\geq 2} a_{\alpha,nm}u^n v^m, \tag{B.7}$$

$$\delta = a_{\delta,01}v + \sum_{n+m\geq 2} a_{\delta,nm}u^n v^m. \tag{B.8}$$

We have verified up to the seventh order that with a proper choice of the coefficients $a_{\alpha,nm}$ and $a_{\delta,nm}$ one can rewrite the β functions in the form

$$\beta_u(u,v) = -uv, \tag{B.9}$$

$$\beta_v(u,v) = -u^2(1 + b_1 v + b_3 v^3 + b_5 v^5 + \cdots). \tag{B.10}$$

The couplings u and v are not uniquely defined and indeed there is a family of transformations that do not change the β functions (B.9) and (B.10). Extending the previous results to all orders, in the following we assume that we can choose u and v in such a way that $\beta_u(u,v)$ is given by (B.9) and $\beta_v(u,v)$ has the form

$$\beta_v(u,v) = -u^2[1 + v f(v^2)], \tag{B.11}$$

where $f(v^2)$ is an analytic function in the region $v < v_0$, where v_0 is the starting point of the RG flow, and satisfies $1 + v f(v^2) > 0$ in this domain (if this were not true, we would have another nontrivial fixed point). This parameterization is unique (universal) in the sense that there is no analytic redefinition of the couplings which allows one to write the β functions in the form (B.9), (B.11) with a different function $f(v^2)$, i.e. with different coefficients b_{2n+1}. The perturbative calculations of [75] allow us to determine b_1:

$$b_1 = -\tfrac{3}{2}. \tag{B.12}$$

J. Stat. Mech. (2010) P03006

The analysis of the flow in the general case is analogous to that presented in [75, 77]. First, we define the RG invariant function

$$Q(u,v) = u^2 - F(v),$$
$$F(v) = 2\int_0^v \frac{w\,\mathrm{d}w}{1+wf(w^2)} = v^2 + v^3 + \frac{9}{8}v^4 + \mathrm{O}(v^5), \tag{B.13}$$

which satisfies

$$\frac{\mathrm{d}Q}{\mathrm{d}l} = \frac{\partial Q}{\partial u}\beta_u(u,v) + \frac{\partial Q}{\partial v}\beta_v(u,v) = 0, \tag{B.14}$$

where l is the flow parameter. The RG flow follows the lines Q = constant. It is thus natural to parameterize the RG flow in terms of Q and $v(l)$. Since

$$\frac{\mathrm{d}v}{\mathrm{d}l} = \beta_v(u,v) = -[Q + F(v)][1 + vf(v^2)], \tag{B.15}$$

we obtain

$$l = -\int_{v_0}^{v} \frac{\mathrm{d}w}{[Q + F(w)][1 + wf(w^2)]}, \tag{B.16}$$

where $v(l=0) = v_0$.

Let us now apply these results to the XY model. Repeating the discussion of [78, 79] the XY model can be mapped onto a line in the (u,v) plane with $v > 0$. The KT transition is the intersection of this line with the line $Q = 0$ and the high-temperature phase corresponds to $Q > 0$. Thus, Q plays the role of thermal nonlinear scaling field, i.e.

$$Q = q_1\tau + q_2\tau^2 + \cdots \tag{B.17}$$

where $\tau = (T - T_{XY})/T_{XY}$.

To derive the expected critical behavior we consider the singular part of the free energy in a box of size L. It satisfies the scaling equation [80]

$$\mathcal{F}_{\mathrm{sing}}(\tau, L) = \mathrm{e}^{-2l} f(Q, v(l), \mathrm{e}^{-l}L), \tag{B.18}$$

where we have parameterized the flow in terms of Q and $v(l)$ and we have neglected all irrelevant operators. If $Q > 0$, as discussed in [75], $v(l)$ decreases continuously and $v(l) \to -\infty$ as $l \to \infty$. Since v_0, the starting point of the flow, is positive, we can fix l by requiring

$$v(l) = -1, \tag{B.19}$$

and so

$$l = \int_{-1}^{v_0} \frac{\mathrm{d}w}{[Q + F(w)][1 + wf(w^2)]} = I(Q, v_0). \tag{B.20}$$

It follows that

$$\mathcal{F}_{\mathrm{sing}}(\tau, L) = \mathrm{e}^{-2I(Q,v_0)} f(Q, -1, \mathrm{e}^{-I(Q,v_0)}L), \tag{B.21}$$

which gives the scaling behavior of the free energy (using $Q \sim \tau$). In the scaling limit the finite-size dependence can be parameterized in terms of ξ/L, where ξ is the correlation

length. This allows us to identify

$$\xi(\tau) = \xi_0 \mathrm{e}^{I(Q,v_0)}, \tag{B.22}$$

where ξ_0 is a constant. The behavior of $\xi(\tau)$ for $\tau \to 0$ is obtained by expanding $I(Q, v_0)$ for $Q \to 0$. The generic behavior is

$$I(Q, v_0) = \frac{1}{\sqrt{Q}} \sum_n I_n Q^n + \sum_n I_{\mathrm{an},n}(v_0) Q^n. \tag{B.23}$$

The nonanalytic terms in the expansion depend only of the coefficients b_{2n+1} which appear in (B.10). The first two coefficients are

$$I_0 = \pi, \qquad I_1 = \frac{\pi b_1}{4} = \frac{9\pi}{16}. \tag{B.24}$$

Correspondingly, we obtain

$$\xi(\tau) = X \exp(\pi/\sqrt{Q})[1 + I_1\sqrt{Q} + \mathrm{O}(Q)]. \tag{B.25}$$

Expanding Q in powers of τ we obtain the celebrated KT expression for the correlation length.

Let us now consider the behavior of the susceptibility. Perturbation theory gives for the scaling dimension of the spin correlation function [75]

$$\gamma = -\tfrac{1}{4} + \tfrac{1}{4}\delta - \tfrac{1}{4}\delta^2 + h_1\alpha^2 + \cdots, \tag{B.26}$$

where h_1 is an unknown coefficient. If we perform the redefinitions $(\alpha, \delta) \to (u, v)$ considered before, we can rewrite γ as[7]

$$\gamma = -\tfrac{1}{4} - \tfrac{1}{8}v - \tfrac{1}{16}v^2 + \cdots \tag{B.27}$$

without the α^2 term. In the infinite-volume limit the susceptibility satisfies the scaling law

$$\chi\xi^{-7/4} = A \exp\left[\int_{v_0}^{v(l)} \frac{\gamma(w) + 1/4}{\beta_v} \mathrm{d}w\right] G_\chi[Q, v(l)], \tag{B.28}$$

the integral is computed at fixed Q with β_v given by (B.15), and G_χ is an analytical function. Setting $v(l) = -1$ and expanding the integral in powers of Q, we obtain an expansion of the form

$$\chi\xi^{-7/4} = A(1 + c_1\sqrt{Q} + c_2 Q + \cdots). \tag{B.29}$$

The coefficient c_1 can be computed exactly using the perturbative results (B.10), (B.12), and (B.27); the result is

$$c_1 = \frac{\pi}{16}. \tag{B.30}$$

[7] The possibility of canceling the term of order α^2 is related to the existence of a family of transformations, given at second order by $u' = u + Auv$, $v' = v + Au^2$ with arbitrary A, which leave invariant the β functions (B.9) and (B.10). By properly choosing A one can eliminate the α^2 term in $\gamma(u', v')$.

J. Stat. Mech. (2010) P03006

Using (B.25) we can write

$$\sqrt{Q} = \frac{\pi}{\ln \xi/X} + \mathrm{O}(\ln^{-3} \xi) \tag{B.31}$$

and obtain

$$\chi \xi^{-7/4} = A_\chi \left[1 + \frac{\pi^2}{16 \ln(\xi/X)} + \mathrm{O}(1/\ln^2 \xi) \right]. \tag{B.32}$$

Note that the leading logarithmic scaling correction has a universal coefficient. We should note that in [77] it was incorrectly claimed that $c_1 = 0$ and, as a consequence, that the leading scaling corrections in (B.32) are proportional to $1/(\ln \xi)^2$. We numerically checked (B.32) by fitting the infinite-volume numerical data of [68] (more precisely their data for $\beta \geq 0.92$, corresponding to $10 \lesssim \xi \lesssim 420$) to

$$\ln(\chi \xi^{-7/4}) = a + \frac{b}{\ln(\xi/X)}; \tag{B.33}$$

the results are $a = 0.804(2)$ and $b = 0.627(9)$ (with $\chi^2/\mathrm{DOF} \approx 0.7$), which are perfectly consistent with the value of b obtained in perturbation theory, i.e. $b = \pi^2/16 \approx 0.617$ (fixing $b = \pi^2/16$, we obtain $a = 0.8058(1)$ with $\chi^2/\mathrm{DOF} \approx 0.7$, while a fit to $a + b/\ln(\xi/X) + c/\ln^2(\xi/X)$ gives $a = 0.8046(9)$, $c = 0.029(22)$ with $\chi^2/\mathrm{DOF} \approx 0.6$, which confirms that the next-to-leading correction is very small in (B.33)).

The result (B.32) is general. If $\mathcal{O}$ is a generic long-distance quantity which behaves as ξ_{o}^x in the critical limit, we expect $\mathcal{O}/\xi_{\mathrm{o}}^x$ to behave as $\chi/\xi^{7/4}$, i.e. to satisfy a relation analogous to (B.28). It is only needed to replace $\gamma(u, v) + 1/4$ with the appropriate subtracted scaling dimension. Thus, $\mathcal{O}/\xi_{\mathrm{o}}^x$ also has an expansion of the form (B.32), i.e.

$$\mathcal{O} = \xi_{\mathrm{o}}^x \left[1 + \frac{c_{\mathcal{O}}}{\ln \xi/X} + \mathrm{O}(\ln^{-2} \xi) \right], \tag{B.34}$$

where $c_{\mathcal{O}}$ is universal and can be computed by using the perturbative expression of the scaling dimension of $\mathcal{O}$. More precisely, if the scaling dimension $\gamma_{\mathcal{O}}(u, v)$ has the perturbative expansion

$$\gamma_{\mathcal{O}}(u, v) = g_{00} + g_{01} v + g_{02} v^2 + g_{20} u^2 + \cdots \tag{B.35}$$

we obtain

$$c_{\mathcal{O}} = -\pi g_{02}. \tag{B.36}$$

Corrections proportional to $1/\ln \xi/X$ should instead be absent in RG invariant quantities. Indeed, if R is such a quantity, if we neglect the scaling corrections, R satisfies the scaling relation

$$R(\tau) = G_R[Q, v(l)], \tag{B.37}$$

for any l. This implies that $R(\tau)$ is independent of $v(l)$, and is hence an analytic function of Q and therefore of τ. It follows that

$$R(\tau) = R^* + \frac{c_R}{\ln^2 \xi/X} + \mathrm{O}(\ln^{-4} \xi), \tag{B.38}$$

where the constant c_R is expected to be universal.

J. Stat. Mech. (2010) P03006

Appendix C. General behavior close to a multicritical point

Let us consider a multicritical point in a two-parameter space labeled by T and σ and let us assume that the correlation length behaves as

$$\xi(T,\sigma) \sim [T - T_{\rm c}(0)]^{-\nu_1} \qquad \sigma = 0, \tag{C.1}$$

$$\xi(T,\sigma) \sim [T - T_{\rm c}(\sigma)]^{-\nu_2} \qquad \sigma > 0, \tag{C.2}$$

where $T_{\rm c}(\sigma)$ is the σ dependent critical point and $\nu_1 \neq \nu_2$. According to the RG, close to the multicritical point $\xi(T,\sigma)$ behaves as

$$\xi(T,\sigma) = u_{\rm t}(T,\sigma)^{-\nu_m} F[u_\sigma(T,\sigma) u_{\rm t}(T,\sigma)^{-\phi}], \tag{C.3}$$

where $u_\sigma(T,\sigma)$ and $u_{\rm t}(T,\sigma)$ are the scaling fields and ϕ and ν_m two critical exponents. Since one of the two scaling fields must vanish along the transition line, we define $u_{\rm t}(T,\sigma)$ as the scaling field which has this property. Therefore, we define

$$u_{\rm t}(T,\sigma) = \frac{T - T_{\rm c}(\sigma)}{T_{\rm c}(0)}. \tag{C.4}$$

For $\sigma \to 0$ and $T \to T_{\rm c}(0)$, it behaves as

$$u_{\rm t}(T,\sigma) = \tau + c_\sigma \sigma + \cdots \qquad \tau \equiv \frac{T - T_{\rm c}(0)}{T_{\rm c}(0)}. \tag{C.5}$$

We assume that $c_\sigma \neq 0$, i.e. that the transition line is not perpendicular to the line $\sigma = 0$, as occurs in the RP XY models. Finally, we note that $u_\sigma(T,\sigma)$ does not vanish on the transition line, unless $\sigma = 0$.

Now consider $T \to T_{\rm c}(\sigma)$ at fixed nonvanishing σ. Since $u_\sigma(T,\sigma) \neq 0$ we obtain (C.2) only if

$$F(x) \sim x^\lambda \qquad \lambda = \frac{\nu_2 - \nu_m}{\phi} \tag{C.6}$$

for $x \to \infty$. To go further let us distinguish two cases: (i) $u_\sigma(T,\sigma)$ vanishes identically for $\sigma = 0$, i.e. $u_\sigma(T,0) = 0$ for any T; (ii) $u_\sigma(T,0)$ is different from zero unless $T = T_{\rm c}(\sigma = 0)$.

In case (i), (C.1) requires

$$F(0) \neq 0, \qquad \nu_m = \nu_1. \tag{C.7}$$

Assuming $u_\sigma(T = T_{\rm c}(0),\sigma) = d_\sigma \sigma$ for $\sigma \to 0$ we obtain

$$\xi(T = T_{\rm c}(0),\sigma) = (c_\sigma \sigma)^{-\nu_1} F(d_\sigma c_\sigma^{-\phi} \sigma^{1-\phi}). \tag{C.8}$$

The observed behavior depends on the value of ϕ. For $\phi < 1$, since $F(0) \neq 0$ we obtain

$$\xi(T = T_{\rm c}(0),\sigma) = (c_\sigma \sigma)^{-\nu_1} (a + b\sigma^{1-\phi} + \cdots). \tag{C.9}$$

The corrections are correct provided that $F(x)$ is analytic for $x = 0$. If $\phi > 1$, using (C.6) we obtain the behavior

$$\xi(T = T_{\rm c}(0),\sigma) \sim \sigma^{-\bar\nu} \qquad \bar\nu = \nu_1 - (1-\phi)\lambda = \frac{\nu_2(\phi - 1) + \nu_1}{\phi}. \tag{C.10}$$

doi:10.1088/1742-5468/2010/03/P03006

J. Stat. Mech. (2010) P03006

In case (ii), if $u_\sigma(T,\sigma=0) = d_T\tau + \mathrm{O}(\tau^2)$ we obtain for $\sigma = 0$

$$\xi(T,0) = \tau^{-\nu_m} F(d_T \tau^{1-\phi}), \tag{C.11}$$

which shows that

$$F(d_T\tau^{1-\phi}) \sim \tau^{\nu_m-\nu_1} \tag{C.12}$$

in the limit $\tau \to 0$. Let us now consider the behavior for $T = T_{\rm c}(0)$ as a function of σ. For $\sigma \to 0$ we have

$$\xi(T = T_{\rm c}(0),\sigma) = c_\sigma^{-\nu_m}\sigma^{-\nu_m} F(d_\sigma c_\sigma^{-\phi}\sigma^{1-\phi}) \sim \sigma^{-\nu_1}, \tag{C.13}$$

where we have used relation (C.12). Thus, in case (ii) we have $\xi(T = T_{\rm c}(0),\sigma) \sim \sigma^{-\nu_1}$ for any value of ϕ.

Let us now show that the case relevant for the RP XY model is case (i). Indeed, case (ii) can only occur if the two relevant operators which occur at the multicritical point are both present in the model at $\sigma = 0$. This certainly does not occur in our case in which σ is associated with randomness. Therefore, our result that in the RP XY model $\xi(T = T_{\rm c}(0),\sigma)$ behaves as $\sigma^{-\nu_1}$ implies that $\phi < 1$, i.e. that the RG dimension of the new operator that arises in the theory with $\sigma \neq 0$ is less relevant than the thermal operator present at $\sigma = 0$. This is also the case for three-dimensional randomly dilute Ising systems or $\pm J$ Ising models at their ferromagnetic transitions at small disorder. Indeed, the crossover from the pure critical behavior to that of the randomly dilute Ising universality class is described by the crossover exponent $\phi = \alpha_{\rm Is} = 0.1096(5)$ [70, 81]; see also the discussion reported in [82].

Similar considerations apply to other quantities. For instance, consider a RG invariant quantity R. It behaves as

$$R(T,\sigma) = r[u_\sigma(T,\sigma) u_{\rm t}(T,\sigma)^{-\phi}]. \tag{C.14}$$

If $\phi < 1$, $R(T,\sigma)$ approaches the same value R^* along the lines $\sigma = 0$ and $T = T_{\rm c}(0)$. Moreover, in the second case we expect corrections of the form

$$R(T_{\rm c}(0),\sigma) = R^* + a\sigma^{1-\phi} + \cdots = R^* + a'\xi^{(\phi-1)/\nu_1} + \cdots. \tag{C.15}$$

Appendix D. RG equations in the presence of randomness

The RG equations in the small disorder regime and close to the paramagnetic–QLRO transition line have been derived in [3, 23, 28, 31, 35]:

$$\frac{{\rm d}T}{{\rm d}l} = -4\pi^3 Y^2, \qquad \frac{{\rm d}\sigma}{{\rm d}l} = 0, \qquad \frac{{\rm d}Y}{{\rm d}l} = (2 - \pi\beta + \pi\sigma\beta^2)Y,$$

where Y is the vorticity and only terms up to $\mathrm{O}(Y^2)$ are kept. Let us now redefine the couplings as follows:

$$T^{-1} = \frac{1}{\pi}(2 + v + \sigma), \qquad Y = \frac{u}{4\pi}. \tag{D.1}$$

For $u, v \to 0$ the RG equations become

$$\frac{{\rm d}u}{{\rm d}l} = -uv, \qquad \frac{{\rm d}v}{{\rm d}l} = -u^2, \qquad \frac{{\rm d}\sigma}{{\rm d}l} = 0. \tag{D.2}$$

We have thus obtained again the RG equations for the XY model. This implies that, in the region of couplings in which (D.2) hold, the RG behavior is analogous to that close to the KT fixed point, apart from an analytic redefinition of the scaling fields.

Appendix E. Magnetic correlations in the gauge-glass model

For the gauge-glass model ($\sigma = \infty$) we can derive some identities which relate magnetic and overlap quantities. The basic observation is that for $\sigma = +\infty$ the distribution function of the A_{xy} variables is gauge invariant. Hence we have

$$[\langle \psi^*_{x_1} \cdots \psi^*_{x_n} \psi_{y_1} \cdots \psi_{y_n} \rangle] = V^*_{x_1} \cdots V^*_{x_n} V_{y_1} \cdots V_{y_n} [\langle \psi^*_{x_1} \cdots \psi^*_{x_n} \psi_{y_1} \cdots \psi_{y_n} \rangle], \tag{E.1}$$

for any set of phases V_x. This implies that magnetic correlations vanish unless each x_i is equal to some y_j. Analogously we have

$$\begin{aligned}[\langle \psi^*_{x_1} \cdots \psi^*_{x_n} \psi_{y_1} \cdots \psi_{y_n} \rangle \langle \psi^*_{z_1} \cdots \psi^*_{z_n} \psi_{\mathrm{t}_1} \cdots \psi_{\mathrm{t}_n} \rangle] &= V^*_{x_1} \cdots V^*_{x_n} V_{y_1} \cdots V_{y_n} V^*_{z_1} \cdots V^*_{z_n} V_{\mathrm{t}_1} \cdots V_{\mathrm{t}_n} \\ &\times [\langle \psi^*_{x_1} \cdots \psi^*_{x_n} \psi_{y_1} \cdots \psi_{y_n} \rangle \langle \psi^*_{z_1} \cdots \psi^*_{z_n} \psi_{\mathrm{t}_1} \cdots \psi_{\mathrm{t}_n} \rangle].\end{aligned} \tag{E.2}$$

These relations allow us to write

$$[\langle \psi^*_x \psi_y \rangle] = \delta_{xy}, \tag{E.3}$$

$$[\langle \psi^*_{x_1} \psi^*_{x_2} \psi_{y_1} \psi_{y_2} \rangle] = \delta_{x_1 y_1} \delta_{x_2 y_2} + \delta_{x_1 y_2} \delta_{x_2 y_1} - \delta_{x_1 y_1} \delta_{x_1 x_2} \delta_{x_1 y_2}, \tag{E.4}$$

$$[\langle \psi^*_{x_1} \psi_{y_1} \rangle \langle \psi^*_{x_2} \psi_{y_2} \rangle] = \delta_{x_1 y_1} \delta_{x_2 y_2} + \delta_{x_1 y_2} \delta_{x_2 y_1} [|\langle \psi^*_{x_1} \psi_{y_1} \rangle|^2] - \delta_{x_1 y_1} \delta_{x_1 x_2} \delta_{x_1 y_2}. \tag{E.5}$$

It follows that

$$[\langle |\mu|^2 \rangle] = V, \qquad [\langle |\mu|^4 \rangle] = 2V^2 - V, \qquad [\langle |\mu|^2 \rangle^2] = V^2 + V^2 \chi_{\mathrm{o}} - V, \tag{E.6}$$

which imply

$$\chi = 1, \qquad \chi_4 = 1 - 2\chi_{\mathrm{o}}, \qquad \chi_{22} = \chi_{\mathrm{o}} - 1. \tag{E.7}$$

Moreover, it is easy to show that $\xi = 0$. Relations (E.7) show that χ_4 and χ_{22} both diverge as χ_{o}. In the critical limit we have $\chi_{\mathrm{o}} \sim \xi^2_{\mathrm{o}}$ because $\eta_{\mathrm{o}} = 0$. Therefore we can write

$$\chi_4 \approx -2a\xi^2_{\mathrm{o}}, \qquad \chi_{22} \approx a\xi^2_{\mathrm{o}}, \tag{E.8}$$

for $\xi_{\mathrm{o}} \to \infty$, where a is constant.

We shall now assume that these results are valid for the whole universality class: for any $\sigma > \sigma_{\mathrm{D}}$, relations (E.8) always hold with a constant a which in general depends on σ. We can re-express these results in terms of the quartic couplings. If we use (E.8) we have

$$g_4 = \frac{3a\xi^2_{\mathrm{o}}}{\chi^2 \xi^2}, \tag{E.9}$$

$$g_{22} = -\frac{a\xi^2_{\mathrm{o}}}{\chi^2 \xi^2}. \tag{E.10}$$

Since the magnetic susceptibility χ and correlation length ξ are finite and nonzero (except for $\sigma = \infty$, where anyway the quartic couplings are not well-defined since $\xi = 0$ for any L), we expect g_4 and g_{22} to diverge as ξ^2_{o} in the critical limit. As for $g_{\mathrm{c}} = g_4 + 3g_{22}$, (E.10) shows that the leading ξ^2_{o} term cancels. Since in the calculation we have neglected the scaling corrections to (E.8), this does not necessarily imply that g_{c} remains finite in the critical limit, but only that $g_{\mathrm{c}} \xi^{-2}_{\mathrm{o}} \to 0$ as $\xi_{\mathrm{o}} \to \infty$. The exact behavior depends on the neglected scaling corrections. These predictions are confirmed by our numerical results; see section 6.7. It is worth mentioning that this behavior is analogous to that observed in the 2D Ising spin glass model, where χ_4 behaves as χ_{o} and thus diverges on approaching the glassy transition; see, e.g., [83] and references therein.

doi:10.1088/1742-5468/2010/03/P03006

J. Stat. Mech. (2010) P03006

References

[1] Granato E and Kosterlitz J M, *Quenched disorder in Josephson-junction arrays in a transverse magnetic field*, 1986 *Phys. Rev.* B **33** 6533

[2] Granato E and Kosterlitz J M, *Disorder in Josephson-junction arrays in a magnetic field*, 1989 *Phys. Rev. Lett.* **62** 823

[3] Rubinstein M, Shrainam B and Nelson D R, *Two-dimensional XY magnets with random Dzyaloshinskii–Moriya interactions*, 1983 *Phys. Rev.* B **27** 1800

[4] Cha M-C and Fertig H A, *Orientational order and depinning of the disordered electron solid*, 1994 *Phys. Rev. Lett.* **73** 870 [arXiv:cond-mat/9402021]
Cha M-C and Fertig H A, *Topological defects, orientational order, and depinning of the electron solid in a random potential*, 1994 *Phys. Rev.* B **50** 14368 [arXiv:cond-mat/9409001]

[5] Fisher M P A, Tokuyasu T A and Young A P, *Vortex variable-range-hopping resistivity in superconducting films*, 1991 *Phys. Rev. Lett.* **66** 2931

[6] Korshunov S E, *Phase transitions in two-dimensional systems with continuous degeneracy*, 2006 *Usp. Fiz. Nauk* **176** 233
Korshunov S E, 2006 *Phys. Usp.* **49** 225 (Engl. Transl.)

[7] Kawashima N and Rieger H, *Recent progress in spin glasses*, 2004 *Frustrated Spin Systems* ed H T Diep (Singapore: World Scientific) [arXiv:cond-mat/0312432]

[8] Ozeki Y and Nishimori H, *Phase diagram of gauge glasses*, 1993 *J. Phys. A: Math. Gen.* **26** 3399

[9] Nishimori H, *Exact results on spin glass models*, 2002 *Physica* A **306** 68 [arXiv:cond-mat/0201056]

[10] Ebner C and Stroud D, *Diamagnetic susceptibility of superconducting clusters: spin-glass behavior*, 1985 *Phys. Rev.* B **31** 165

[11] Forrester M G, Lee H J, Tinkhams M and Lobb C J, *Positional disorder in Josephson-junction arrays: experiments and simulations*, 1988 *Phys. Rev.* B **37** 5966

[12] Chakrabarti A and Dasgupta C, *Phase transition in positionally disordered Josephson-junction arrays in a transverse magnetic field*, 1988 *Phys. Rev.* B **37** 7557

[13] Forrester M G, Benz S P and Lobb C J, *Monte Carlo simulations of Josephson-junction arrays with positional disorder*, 1990 *Phys. Rev.* B **41** 8749

[14] Huse D A and Seung H S, *Possible vortex-glass transition in a model random superconductor*, 1990 *Phys. Rev.* B **42** 1059

[15] Reger J D, Tokuyasu T A, Young A P and Fisher M P A, *Vortex-glass transition in three dimensions*, 1991 *Phys. Rev.* B **44** 7147

[16] Li Y-H, *Voltage–current characteristics of the two-dimensional gauge glass model*, 1992 *Phys. Rev. Lett.* **69** 1819

[17] Gingras M J P, *Numerical study of vortex-glass order in random-superconductor and related spin-glass models*, 1992 *Phys. Rev.* B **45** 7547

[18] Dekker C, Wöltgens P J M, Koch R H, Hussey B W and Gupta A, *Absence of a finite-temperature vortex-glass phase transition in two-dimensional* $YBa_2Cu_3O_{7-\delta}$ *films*, 1992 *Phys. Rev. Lett.* **69** 2717

[19] Reger J D and Young A P, *Monte Carlo study of a vortex glass model*, 1993 *J. Phys. A: Math. Gen.* **26** L1067 [arXiv:cond-mat/9311036]

[20] Korshunov S E, *Possible destruction of the ordered phase in Josephson-junction arrays with positional disorder*, 1993 *Phys. Rev.* B **48** 1124

[21] Nishimori H and Kawamura H, *Gauge glass ordering in two dimensions*, 1993 *J. Phys. Soc. Japan.* **62** 3266

[22] Nishimori H, *Gauge glass, spin glass and coding theory: Exact results*, 1994 *Physica* A **205** 1

[23] Nattermann T, Scheidl S, Korshunov S E and Li M S, *Absence of reentrance in the two-dimensional XY model with random phase shifts*, 1995 *J. Physique* I **5** 565 [arXiv:cond-mat/9501120]

[24] Cha M-C and Fertig H A, *Disorder-induced phase transitions in two-dimensional crystals*, 1995 *Phys. Rev. Lett.* **74** 4867

[25] Jeon G S, Kim S and Choi M Y, *Phase transition in the XY gauge glass*, 1995 *Phys. Rev.* B **51** 16211

[26] Hyman R A, Wallin M, Fisher M P A, Girvin S M and Young A P, *Current–voltage characteristics of two-dimensional vortex-glass models*, 1995 *Phys. Rev.* B **51** 15304 [arXiv:cond-mat/9409117]

[27] Korshunov S E and Nattermann T, *Absence of reentrance in superconducting arrays with positional disorder*, 1996 *Phys. Rev.* B **53** 2746

[28] Tang L-H, *Vortex statistics in a disordered two-dimensional XY model*, 1996 *Phys. Rev.* B **54** 3350 [arXiv:cond-mat/9602162]

[29] Bokil H S and Young A P, *Study of chirality in the two-dimensional XY spin glass*, 1996 *J. Phys. A: Math. Gen.* **29** L89 [arXiv:cond-mat/9512042]

J. Stat. Mech. (2010) P03006

[30] Maucourt J and Grempel D R, *Phase transitions in the two-dimensional XY model with random phases: a Monte Carlo study*, 1997 *Phys. Rev.* B **56** 2572 [arXiv:cond-mat/9703109]
[31] Scheidl S, *Glassy vortex state in a two-dimensional disordered XY model*, 1997 *Phys. Rev.* B **55** 457 [arXiv:cond-mat/9601131]
[32] Kosterlitz J M and Simkin M V, *Numerical study of a superconducting glass model*, 1997 *Phys. Rev. Lett.* **79** 1098 [arXiv:cond-mat/9702166]
[33] Kim B J, Choi M Y, Ryu S and Stroud D, *Anomalous relaxation in the XY gauge glass*, 1997 *Phys. Rev.* B **56** 6007 [arXiv:cond-mat/9707140]
[34] Maucourt J and Grempel D R, *Scaling of domain-wall energies in the three-dimensional gauge glass model*, 1998 *Phys. Rev.* B **58** 2654
[35] Carpentier D and Le Doussal P, *Disordered XY models and Coulomb gases: renormalization via traveling waves*, 1998 *Phys. Rev. Lett.* **81** 2558 [arXiv:cond-mat/9802083]
[36] Granato E, *Current–voltage scaling of chiral and gauge-glass models of two-dimensional superconductors*, 1998 *Phys. Rev.* B **58** 11161 [arXiv:cond-mat/9808331]
[37] Sawa A, Yamasaki H, Mawatari Y, Obara H, Umeda M and Kosaka S, *Thickness dependence of the vortex-glass transition and critical scaling of current–voltage characteristics in* $YBa_2Cu_3O_{7-\delta}$ *thin films*, 1998 *Phys. Rev.* B **58** 2868
[38] Kosterlitz J M and Akino N, *Numerical study of spin and chiral order in a two-dimensional XY spin glass*, 1999 *Phys. Rev. Lett.* **82** 4094 [arXiv:cond-mat/9806339]
[39] Mudry C and Wen X-G, *Does quasi-long-range order in the two-dimensional XY model really survive weak random phase fluctuations?*, 1999 *Nucl. Phys.* B **549** 613 [arXiv:cond-mat/9712146]
[40] Choi M Y and Park S Y, *Phase transition in the two-dimensional gauge glass*, 1999 *Phys. Rev.* B **60** 4070 [arXiv:cond-mat/9906326]
[41] Kim B J, *Finite-temperature resistive transition in the two-dimensional XY gauge glass model*, 2000 *Phys. Rev.* B **62** 644 [arXiv:cond-mat/0004069]
[42] Carpentier D and Le Doussal P, *Topological transitions and freezing in XY models and Coulomb gases with quenched disorder: renormalization via traveling waves*, 2000 *Nucl. Phys.* B **588** 565 [arXiv:cond-mat/9908335]
[43] Akino N and Kosterlitz J M, *Domain wall renormalization group study of the XY model with quenched random phase shifts*, 2002 *Phys. Rev.* B **66** 054536 [arXiv:cond-mat/0203299]
[44] Holme P and Olsson P, *A zero-temperature study of vortex mobility in two-dimensional vortex glass models*, 2002 *Europhys. Lett.* **60** 439 [arXiv:cond-mat/0111555]
[45] Katzgraber H G and Young A P, *Numerical studies of the two- and three-dimensional gauge glass at low temperature*, 2002 *Phys. Rev.* B **66** 224507 [arXiv:cond-mat/0205206]
[46] Katzgraber H G, *On the existence of a finite-temperature transition in the two-dimensional gauge glass*, 2003 *Phys. Rev.* B **67** 180402(R) [arXiv:cond-mat/0305393]
Katzgraber H G, *Numerical studies of the two-and three-dimensional gauge glass at low temperature*, 2003 *J. Appl. Phys.* **93** 7661 [arXiv:cond-mat/0304540]
[47] Holme P, Kim B J and Minnhagen P, *Phase transitions in the two-dimensional random gauge XY model*, 2003 *Phys. Rev.* B **67** 104510 [arXiv:cond-mat/0301279]
[48] Chen Q-H, Tanaka A and Hu X, *Evidence for finite-temperature glass transition in two dimensions*, 2003 *Physica* B **329** 1413
[49] Nikolaou M and Wallin M, *Zero-temperature glass transition in the two-dimensional gauge glass model*, 2004 *Phys. Rev.* B **69** 184512 [arXiv:cond-mat/0312066]
[50] Katzgraber H G and Campbell I A, *Dynamical scaling in Ising and vector spin glasses*, 2005 *Phys. Rev.* B **72** 014462 [arXiv:cond-mat/0504082]
[51] Tang L-H and Tong P, *Zero-temperature criticality in the two-dimensional gauge glass model*, 2005 *Phys. Rev. Lett.* **94** 207204 [arXiv:cond-mat/0412415]
[52] Um J, Kim B J, Minnaghen P, Choi M Y and Lee S-I, *Dynamic critical behaviors in two-dimensional Josephson junction arrays with positional disorder*, 2006 *Phys. Rev.* B **74** 094516 [arXiv:cond-mat/0608390]
[53] Yun Y J, Baek I C and Choi M Y, *Experimental study of positionally disordered Josephson junction arrays*, 2006 *Europhys. Lett.* **76** 271 [arXiv:cond-mat/0509151]
[54] Chen Q-H, Lv J-P and Liu H, *Dynamics of glass phases in the two-dimensional gauge glass model*, 2008 *Phys. Rev.* B **78** 054519 arXiv:0812.2822
[55] Alba V, Pelissetto A and Vicari E, *Quasi-long-range order in the 2D XY model with random phase shifts*, 2009 *J. Phys. A: Math. Theor.* **42** 295001 [arXiv:0901.4682]

J. Stat. Mech. (2010) P03006

[56] Ristivojevic Z, *Superconducting film with randomly magnetized dots: a realization of the two-dimensional XY model with random phase shifts*, 2009 *Phys. Rev.* B **80** 174528 [arXiv:0903.5514]

[57] Kosterlitz J M and Thouless D J, *Ordering, metastability and phase transitions in two-dimensional systems*, 1973 *J. Phys. C: Solid State Phys.* **6** 1181

[58] Hasenbusch M and Pinn K, *Computing the roughening transition of Ising and solid-on-solid models by BCSOS model matching*, 1997 *J. Phys. A: Math. Gen.* **30** 63 [arXiv:cond-mat/9605019]
Hasenbusch M, Marcu M and Pinn K, *High-precision renormalization-group study of the roughening transition*, 1994 *Physica* A **208** 124 [arXiv:hep-lat/9404016]

[59] Nishimori H, *Internal energy, specific heat and correlation function of the bond-random Ising model*, 1981 *Prog. Theor. Phys.* **66** 1169

[60] Hasenbusch M, Parisen Toldin F, Pelissetto A and Vicari E, *Multicritical Nishimori point in the phase diagram of the $\pm J$ Ising model on a square lattice*, 2008 *Phys. Rev.* E **77** 051115 [arXiv:0803.0444]

[61] Picco M, Honecker A and Pujol P, *Strong disorder fixed points in the two-dimensional random-bond Ising model*, 2006 *J. Stat. Mech.* P09006 [arXiv:cond-mat/0606312]

[62] Hasenbusch M, Parisen Toldin F, Pelissetto A and Vicari E, *Universal dependence on disorder of two-dimensional randomly diluted and random-bond $\pm J$ Ising models*, 2008 *Phys. Rev.* E **78** 011110 [arXiv:0804.2788]

[63] Parisen Toldin F, Pelissetto A and Vicari E, *Strong-disorder paramagnetic–ferromagnetic fixed point in the square-lattice $\pm J$ Ising model*, 2009 *J. Stat. Phys.* **135** 1039 [arXiv:0811.2101]

[64] Parisen Toldin F, Pelissetto A and Vicari E, 2010 in preparation

[65] Amoruso C and Hartmann A K, *Domain-wall energies and magnetization of the two-dimensional random-bond Ising model*, 2004 *Phys. Rev.* B **70** 134425 [arXiv:cond-mat/0401464]

[66] Wang C, Harrington J and Preskill J, *Confinement-Higgs transition in a disordered Gauge theory and the accuracy threshold for quantum memory*, 2003 *Ann. Phys., NY* **303** 31 [arXiv:quant-ph/0207088]

[67] Campostrini M, Pelissetto A, Rossi P and Vicari E, *Strong-coupling analysis of two-dimensional O(N) models with $N \leq 2$ on square, triangular, and honeycomb lattices*, 1996 *Phys. Rev.* B **54** 7301 [arXiv:hep-lat/9603002]

[68] Balog J, Niedermaier M, Niedermayer F, Patrascioiu A, Seiler E and Weisz P, *Does the XY model have an integrable continuum limit?*, 2001 *Nucl. Phys.* B **618** 315 [arXiv:hep-lat/0106015]

[69] Pelissetto A and Vicari E, *The effective potential of N-vector models: a field-theoretic study to $O(\epsilon^3)$*, 2000 *Nucl. Phys.* B **575** 579 [arXiv:cond-mat/9911452]
Pelissetto A and Vicari E, *Four-point renormalized coupling constant and Callan–Symanzik β-function in $O(N)$ models*, 1998 *Nucl. Phys.* B **519** 123 [arXiv:cond-mat/9711078]

[70] Pelissetto A and Vicari E, *Critical phenomena and renormalization-group theory*, 2002 *Phys. Rep.* **368** 549 [arXiv:cond-mat/0012164]

[71] Geyer C J, *Markov chain Monte Carlo maximum likelihood*, 1991 *Computer Science and Statistics: Proc. of the 23rd Symp. on the Interface* ed E M Keramidas (Fairfax Station, VA: Interface Foundation) p 156
Hukushima K and Nemoto K, *Exchange Monte Carlo method and application to spin glass simulations*, 1996 *J. Phys. Soc. Japan* **65** 1604

[72] Earl D J and Deem M W, *Parallel tempering: theory, applications, and new perspectives*, 2005 *Phys. Chem. Chem. Phys.* **7** 3910 [arXiv:physics/0508111]

[73] Hasenbusch M, Pelissetto A and Vicari E, *Critical behavior of three-dimensional Ising spin glass models*, 2008 *Phys. Rev.* B **78** 214205 [arXiv:0809.3329]
Hasenbusch M, Pelissetto A and Vicari E, *The critical behavior of 3D Ising spin glass models: universality and scaling corrections*, 2008 *J. Stat. Mech.* L02001 [arXiv:0710.1980]

[74] Hasenbusch M, Parisen Toldin F, Pelissetto A and Vicari E, *The universality class of 3D site-diluted and bond-diluted Ising systems*, 2007 *J. Stat. Mech.* P02016 [arXiv:cond-mat/0611707]

[75] Amit D J, Goldschmidt Y Y and Grinstein G, *Renormalisation group analysis of the phase transition in the 2D Coulomb gas, sine–Gordon theory and XY-model*, 1980 *J. Phys. A: Math. Gen.* **13** 585

[76] Balog J and Hegedüs A, *Two-loop beta-functions of the sine–Gordon model*, 2000 *J. Phys. A: Math. Gen.* **33** 6543 [arXiv:hep-th/0003258]

[77] Balog J, *Kosterlitz–Thouless theory and lattice artifacts*, 2001 *J. Phys. A: Math. Gen.* **34** 5237 [arXiv:hep-lat/0011078]

[78] Kosterlitz J M, *The critical properties of the two-dimensional xy model*, 1974 *J. Phys. C: Solid State Phys.* **7** 1046

[79] José J V, Kadanoff L P, Kirkpatrick S and Nelson D R, *Renormalization, vortices, and symmetry-breaking perturbations in the two-dimensional planar model*, 1978 *Phys. Rev.* B **16** 1217

J. Stat. Mech. (2010) P03006

[80] Wegner F J, 1976 *The Critical State* (*General Aspects in Phase Transitions and Critical Phenomena* vol 6) ed C Domb and M Green (New York: Academic) p 7
[81] Campostrini M, Pelissetto A, Rossi P and Vicari E, *25th-order high-temperature expansion results for three-dimensional Ising-like systems on the simple-cubic lattice*, 2002 *Phys. Rev.* E **65** 066127 [arXiv:cond-mat/0201180]
[82] Hasenbusch M, Parisen Toldin F, Pelissetto A and Vicari E, *Magnetic-glassy multicritical behavior of the three-dimensional $\pm J$ Ising model*, 2007 *Phys. Rev.* B **76** 184202 arXiv:0707.2866
[83] Binder K and Young A P, *Spin glasses: experimental facts, theoretical concepts, and open questions*, 1986 *Rev. Mod. Phys.* **58** 801